Deltares

Enabling Delta Life

Quick-scan runup reduction through coral reef restoration in the Seychelles

GFDRR

Global Facility for Disaster Reduction and Recovery

THE WORLD BANK

IBRD • IDA | WORLD BANK GROUP

Quick-scan runup reduction through coral reef restoration in the Seychelles

Stuart Pearson
Marlies van der Lugt
Ap van Dongeren
Gerben Hagenaars
Andreas Burzel

Deltares

Title
Quick-scan runup reduction through coral reef restoration in the Seychelles

Client	Project	Reference	Pages
World Bank	11202446-000	11202446-000-ZKS-0002	54

Keywords
Coastal hazards, coral reefs, small island developing state, waves, wave runup, coral restoration

Summary
The World Bank is initiating a project in the Seychelles on coral restoration to prevent coastal flooding. Deltares has been requested to perform a quick-scan analysis to select priority sites with high coastal flood risk, and high potential for flood risk reduction through coral restoration around the three main islands of Mahé, La Digue and Praslin. Coral restoration is a prime candidate to reduce marine flooding as mean coral cover has reduced to less than 11% of the historic cover after the 1998 El Nino bleaching.

The objective is to perform a quick-scan analysis for three islands of the Seychelles to identify candidate sites which have a high potential for the reduction of wave runup through coral reef restoration. Wave runup is selected as a proxy for coastal flooding levels. This quick-scan analysis will be carried out first using remote sensing and existing datasets to estimate key site parameters such as reef width, depth, roughness, and beach slope. Hydrodynamic forcing will be assessed using wave and water level conditions prescribed by the client. The reef morphology and hydrodynamic forcing will then be used in the BEWARE system to estimate runup under a range of different scenarios, including reef roughness as a proxy for coral health.

The end products of this project are spatial maps of relative and absolute runup change for the three islands for various water levels and wave conditions, together with the digital data of the computed runup values. Intermediate data on the reef input parameters (reef width, reef slope, beach slope, and reef roughness) are also included. This information may guide the selection of candidate sites for coral reef restoration.

Handling and document control
Prepared by Deltares:

Authors: Stuart Pearson, Marlies van der Lugt, Ap van Dongeren, Gerben Hagenaars, Andreas Burzel
Review: Kees Nederhoff
Approval: Frank Hoozemans

Quality control and review by World Bank:

Task Team: Brenden Jongman, Boris Ton Van Zanten

This online version of the report is based on the Deltares report 11202446-000-ZKS-0001. The original report has been adjusted to fit the requirements of the World Bank for online publication. The signatures for approval of the original report have therefore been omitted. Besides the adjustments to the format and the absence of signatures the content of the original Deltares report 11202446-000-ZKS-0001 has not been altered or adjusted in any manner or form.

Contents

Figures

Tables

1 Introduction[1]

The Global Facility for Disaster Reduction and Recovery (GFDRR) is a partnership of the World Bank, United Nations, major donors and recipient countries under the International Strategy for Disaster Reduction (ISDR) system to support the implementation of the Hyogo Framework for Action (HFA). Launched in September 2006, GFDRR provides technical and financial assistance to help disaster-prone countries decrease their vulnerability and adapt to climate change. GFDRR works closely with UN agencies, client governments, World Bank regional offices, and other partners. GFDRR implements the majority of its activities in countries through the World Bank, in partnership with national, regional, and other international agencies. It is organized along three tracks of operation to achieve its development objectives at the global, regional and country levels.

To meet the needs of a rapidly changing world, GFDRR Innovation Lab supports the use of science, technology, and open data in promoting new ideas and the development of original tools to empower decision-making in vulnerable countries to strengthen their resilience. Recent innovations in the field have enabled better access to disaster and climate risk information and a greater capacity to create, manage, and use this information. Innovation Lab activities are designed and implemented in partnership with government institutions and key international and local partners, ensuring that all activities add value in planning, operational, and recovery activities.

In December 2013, as part of the European Unions' (EU) cooperation with Africa, Caribbean and Pacific countries, the EU approved a €60 million contribution to support the development of an analytical basis for risk financing and to accelerate the effective implementation of a comprehensive disaster risk reduction entitled "Building Disaster Resilience to Natural Hazards in Sub-Saharan African Regions, Countries and Communities". The World Bank's Global Facility for Disaster Reduction and Recovery (GFDRR) was selected as the implementing partner of the Program for Result Area 5: the "Africa Disaster Risk Assessment and Financing Program." This component aims to support the development of multi-risk financing strategies developed at regional, national, and local levels to help African countries make informed decisions to improve their financial response capacity post-disaster and to mitigate the socio-economic, fiscal and financial impacts of disasters.

Being a small island nation, the Seychelles are highly exposed to natural hazards, especially coastal erosion, coastal flooding, flash flooding and rock fall. To efficiently prepare for, respond to, and finance these risks, it is important to have a comprehensive understanding of hazards, exposure and vulnerability.

In an effort to improve this understanding and explore potential sites for nature-based solutions – in the form coral reef restoration in particular – to reduce coastal flood risk, the GFDRR and World Bank contracted Deltares for a quick scan analysis to inform the selection of priority sites with high coastal flood risk, and high potential for flood risk reduction through coral restoration around the three main islands of Mahé, La Digue and Praslin. Coral restoration is a prime candidate to reduce marine flooding as mean coral cover has reduced to less than 11% of the historic cover after the 1998 El Nino bleaching.

[1] *Most of this text is taken from the World Bank provided text in the Contract.*

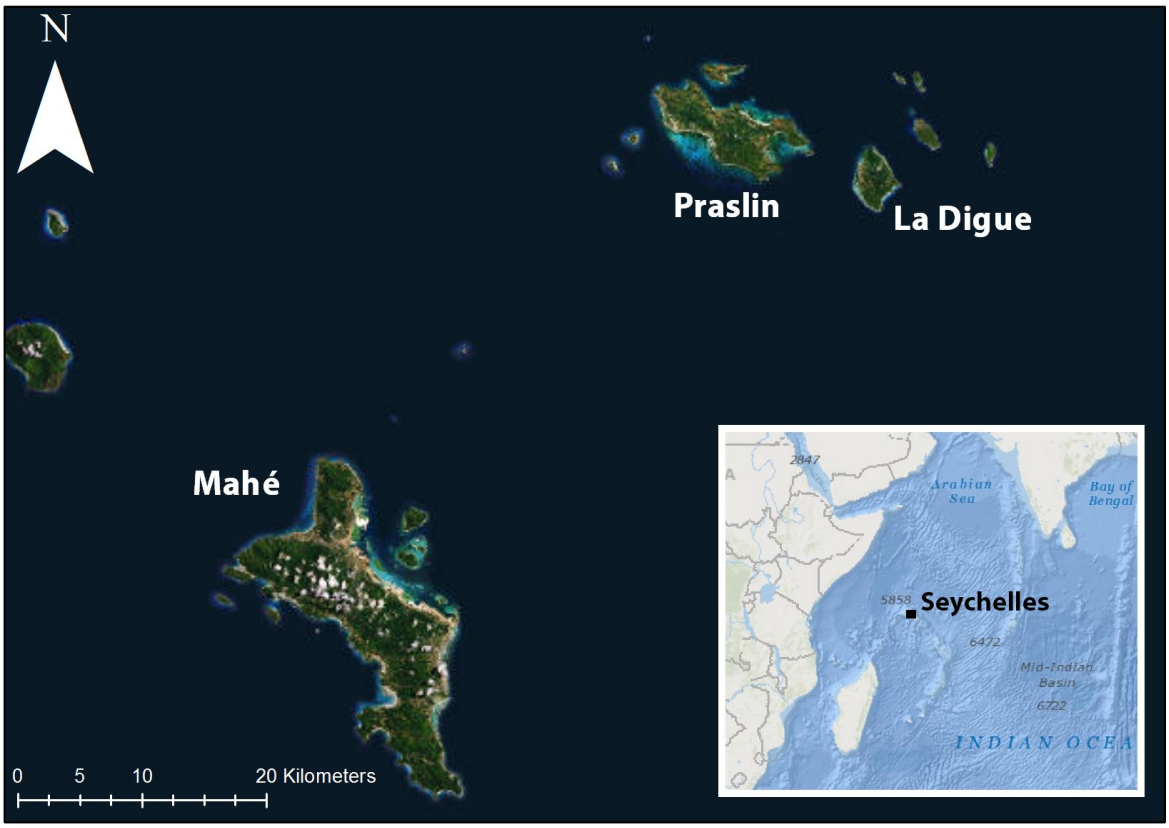

Figure 1.1 Location of the three sites of interest in the Seychelles: Mahé, Praslin, and La Digue.

2 Objective and limitations

The objective of this study is to perform a quick-scan analysis for three islands of the Seychelles to identify candidate sites which have a high potential for the reduction of wave runup through coral reef restoration. Wave runup is selected as a proxy for coastal flooding levels.

The quick scan analysis method was selected due to limited time, limited funding and more importantly limited data that would be needed to perform a full-scale analysis. This implies that in potential later stages of the project, additional data and analysis is required to make the analysis more robust.

3 Method

In this study, we apply the recently published BEWARE (Bayesian Estimator of Wave Attack in Reef Environments) system to the islands Pearson et al. (2017a). The system computes the hazard of runup as a function of the offshore forcing (wave height, wave steepness and water level) and the geometric properties of the reef (width, reef slope, beach slope, and roughness). The forcing and geometric properties are required inputs into the model which need to be obtained from either literature, direct measurements or through remote sensing. In this project, we elected to obtain the geometric properties through satellite image interpretation and the hydrodynamic properties from literature as it is not feasible to measure directly in the field for a prolonged period of time and at many locations.

3.1 BEWARE method

The BEWARE system uses the results of a validated process-based numerical wave model were combined with a probabilistic Bayesian network. Several steps were carried out by Pearson et al. (2017a) to initially develop the BEWARE system:

1. Schematize the reef and forcing conditions, and formulate a range of input parameters based on field measurements and typical values from the literature.

2. Simulate nearshore hydrodynamics for the full range of parameters using the validated process-based wave and water level XBeach Non-Hydrostatic (XBHN) model (Smit et al., 2010) to create a synthetic database of hydrodynamic responses to extrinsic forcing and intrinsic coral reef geomorphology (Pearson et al., 2017b).

3. Develop a Bayesian network and train with model results.

4. Validate the Bayesian network by comparing predictions to field observations.

5. Assess the performance of the Bayesian network using techniques such a log likelihood ratios and confusion matrices.

Given suitable input conditions, the BEWARE system is then ready for use in making predictions of runup. For this project, the hydrodynamic forcing and reef geometry exceeded the bounds of the original BEWARE parameter space, and therefore, additional XBNH simulations were carried out to populate the database.

3.2 Determine cross-shore transects

The geometric properties of the reef (such as reef flat widths and fore reef slopes) are determined along cross-shore transects. First, “splines” or contours are drawn around each island which roughly follow the shape of the island. Then, cross-shore transects are constructed perpendicular to the spline at approximately 250 meter intervals. This resolution is sufficient to characterize the essential features of the coastline, without attempting to provide more detail than the available (remote sensing) data permits. The transects cover most of the island coast, but do not include areas with rocky cliffs, sandy coves with shorebreaks (which are an indication of steep bathymetry), sections of the coastline that are sheltered by offshore islands, or uninhabited areas.

3.3 Obtain reef widths

Along the transects, reef widths are obtained using satellite imagery from Sentinel 2. Here, the reef width is defined as the distance between the shoreline position and the position of wave breaking at the offshore edge of the reef (i.e. the transition between the fore reef and reef crest in Figure 3.1). The shoreline position is found by using a land-water detection method based on the Normalized Difference Water Index (NDWI) indicator, defined as:

$$NDWI = \frac{\lambda_{NIR} - \lambda_{GREEN}}{\lambda_{NIR} + \lambda_{GREEN}}$$

in which λ_{NIR} is the energy reflectance per pixel in the Near InfraRed (NIR) band and λ_{NIR} is the energy reflectance in the Green band. For additional details on this method, see Hagenaars et al. (2018).

The outer reef edge position will be determined using the NIR signal, which is sensitive to foam, indicative of wave breaking. At the location of wave breaking a clear peak in NIR on the seaward side of the transect is expected, and an algorithm to automatically detect the location of this peak on seven cloud-free 2017 and 2018 Sentinel 2 images is used. All these images were obtained from October until June, which is the Southern hemisphere summer when the prevailing wave forcing is low. The average peak NIR location is then used as the reef edge, which in combination with the shoreline, defines the reef width for each transect. The standard deviation of the peak NIR locations is also stored.

3.4 Obtain beach slopes

Beach slopes are obtained from overlaying the transects onto the Digital Terrain Model (DTM) as provided by World Bank. The beach slope will be estimated by calculating a moving multi-point average of the terrain elevation over a certain length, which is a standard filter technique in raster GIS operations (Demers, 2008; Grohmann & Riccomini, 2009; Lillesand et al. 2014). This method allows for the consideration of existing noise in the terrain model and returns an averaged beach slope for the runup calculations.

3.5 Obtain hydrodynamic forcing

The next step is to obtain the offshore water levels and wave heights that drive flooding on the shore.

3.5.1 Water levels

A report provided by the Client (Japan International Cooperation Agency, 2014) includes design water levels for different return periods, accounting for changes in sea level. The relative contribution of sea level rise and storm surge is not specified. Based on the availability of wave data, a return period of 1/25 years is selected to perform the analysis.

Table 3.1 25-year return period water levels for analysis (Japan International Cooperation Agency, 2014).

Target Year	**2010**	**2050**	**2100**
Water Level [m above]	1.44	1.70	2.03

3.5.2 Wave heights & periods

The provided data by the World Bank does not give a complete estimate of the normative wave heights around the islands. At the Seychelles, wave heights vary according to the season and are affected by tropical cyclones (which are not included in wave climate databases). Since a

wave climate analysis requires a beyond scope effort, we use the normative wave heights (1/25 year return period) as shown in Table 3.2 below (Japan International Cooperation Agency, 2014). These wave heights are up to 30% higher (more conservative) than the wave heights estimated at the North-East Point (Borrero et al., 2016)

Table 3.2 25-year return period wave conditions for analysis (Japan International Cooperation Agency, 2014). The wave directions are stated for completeness but are not used in the analysis, as all waves are assumed to propagate parallel to the transect.

Island	Location	Wave Height [m]	Wave Period [s]	Wave Direction [-]
Mahé	North East Point	4.0	8.0	ESE
	Au Cap	5.0	8.0	SSE
	Anse Royale	5.0	8.0	ESE
	Baie Lazare	4.0	7.0	SSW
Praslin	Anse Kerlan	4.0	7.0	SSW
La Digue	La Passe	4.0	6.0	WSW

The conditions for the waves and water levels form the “base cases” for which the runup is calculated. To supplement the normative wave conditions, additional scenarios will be tested to demonstrate the sensitivity of runup to different wave heights (-1 m and + 2 m).

These design wave conditions exceed the current BEWARE parameter space, so additional model runs will be conducted to approximate the full range of expected forcing.

3.6 Assess reef elevation

The mean water depth over the reefs are estimated from Landsat 8 images using the aerosol, blue and green bands according to the regression method described in (Pacheco et al., 2015). In order to refine the image pixel resolution (30 meter), the bands are interpolated using bi-cubic resampling. The depth estimation technique will return an unreferenced water depth, as it does not relate this depth to a vertical datum. In order to correct the water levels (and thus reef elevations), an analysis including the contribution of the tidal water level and wave setup that were present at the time of satellite image acquisition would be required. For this quick-scan analysis, we assume that the wave conditions at the time of image recording are small and thus that the wave-induced setup is small as well. For incident wave heights of 1 m, Pearson et al. (2017) finds a mean wave-induced setup of 0.07 m, which is small (<10%) relative to the total water depth over the reef due to the tidal elevation and reef elevation. This means that we can relate the water level estimation only to the tidal water level, obtained using the Topex Poseidon 8.0 global tide dataset at a location close to the coastal site. We will then use this information to reference the satellite observed water level to mean sea level (MSL) and then use the water depth to estimate the reef elevation relative to MSL.

Based on the obtained reef elevation the average reef depth (defined as the average of the depths in between the shoreline and the point of wave breaking) and the offshore slope (defined as the slope based on linear regression of the elevations between the point of wave breaking and the -7 m depth contour) are retrieved and used as input for the BEWARE analysis. The depth at the position of wave breaking is also stored per transect. This method assumes that the reef transect in question has a typical fringing reef shape similar to Figure 3.1, with a broad reef flat and abrupt change in bathymetry at the reef crest.

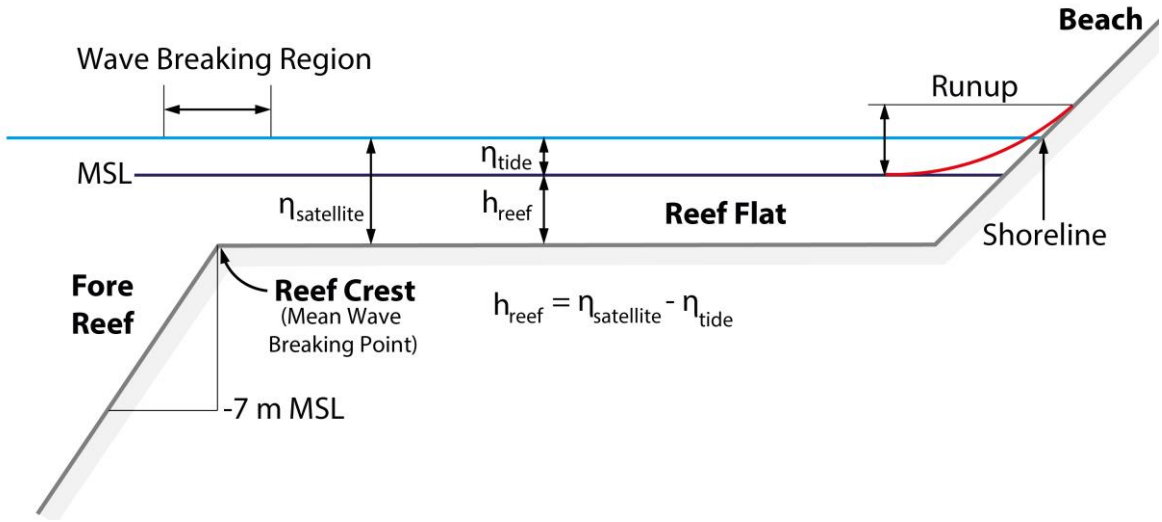

Figure 3.1 Schematization of reef flat elevation estimate. The average depth on the reef flat (h_{reef}) is calculated by subtracting the tidal elevation at the time of the satellite image (η_{tide}) from the satellite-estimated depth on the reef ($\eta_{satellite}$).The reef crest is defined as the mean wave breaking point, and the fore reef slope is derived based on the elevations between this crest and the -7 m depth contour.

We will compare the obtained reef elevations at a selection of sites with the bathymetric surveys provided by the client, where sufficient data is readily available. However, in our experience from other tropical areas, surveyed reef elevations are usually inaccurate, and thus these measurements will be used primarily to help interpret the data obtained via remote sensing where available.

Uncertainty in the remote sensing depth estimation is quantified by performing the depth retrieval algorithm for the range of calibration factors described (Pacheco et al., 2015).

3.7 Assess current reef rugosity

Reef rugosity (roughness) is an input into the BEWARE model, which governs the wave height attenuation (decay) over the reef. The rugosity is related to the "structural complexity" of the corals. Numerous previous studies (e.g. Sheppard et al., 2005; Baldock et al., 2014; Harris et al., 2018) have equated damaged or dead coral with a reduced hydrodynamic roughness. However, quantitative data on structural complexity is very scarce, as is detailed data of past and present coral coverage. Therefore, the sensitivity of the model to a range of roughness coefficients, representing the relative degrees of coral coverage, is examined in a range of c_f = 0.001 (equivalent to a sandy beach with no coral), c_f = 0.01 (low coral cover and roughness), c_f = 0.05 (medium roughness) to c_f = 0.1 (high coral coverage with complex structures). These values were selected based on previous modelling studies in coral environments (e.g. Quataert et al., 2015).

This will give insight into the *flood-reduction potential* of a coral reef in a given transect: how much will runup reduce with an increase in hydrodynamic roughness? At transects with high potential, the historical and current status of the live coral cover becomes relevant from a flood risk perspective and should be investigated further. This is beyond the scope of this quick-scan study. The above parameters will be used to constrain the computed runup in BEWARE per coastal transect.

3.8 Assess and visualize absolute runup changes as a function of changes in reef health.

Using reef roughness as a proxy for reef health, we compare the absolute reduction of the runup as reef roughness parameters are changed from no roughness to low, medium, and high using the BEWARE tool and indicate areas with high potential runup reduction.

4 Results

4.1 Cross-shore transects

The first step in obtaining the reef width is to define alongshore splines (e.g. green line in Figure 4.3) and cross-shore transects at approximately 250 meters distance as shown in Figure 4.1. The transects cover most of the island coast, but do not include areas with rocky cliffs, sandy coves with shorebreaks (which are an indication of steep bathymetry), sections of the coastline that are sheltered by offshore islands, or unoccupied areas. These omitted areas are estimated to have little potential for reef presence. A total of 308 transects (40 on La Digue, 173 on Mahé, and 95 on Praslin) are defined for this study. All of the priority areas as defined by Seychelles Ministry of the Environment are within the analysed area (Boris van Zanten, World Bank, personal communication), except Anse Boudin on Praslin Island, which is located in a sheltered area.

The islands of La Digue, Mahé and Praslin are subdivided into coastal sites with a unique name. This results in coastal sites D0 for La Digue, M0 up to M8 for Mahé (numbered clockwise, starting north with the exception of M8) and P0 up to P4 for Praslin (numbered clockwise starting east). Each transects has a unique identifier, named as: *Island_site_transectnumber* (e.g. *Mahé_M1_0* for the first transect at Mahé site M1).

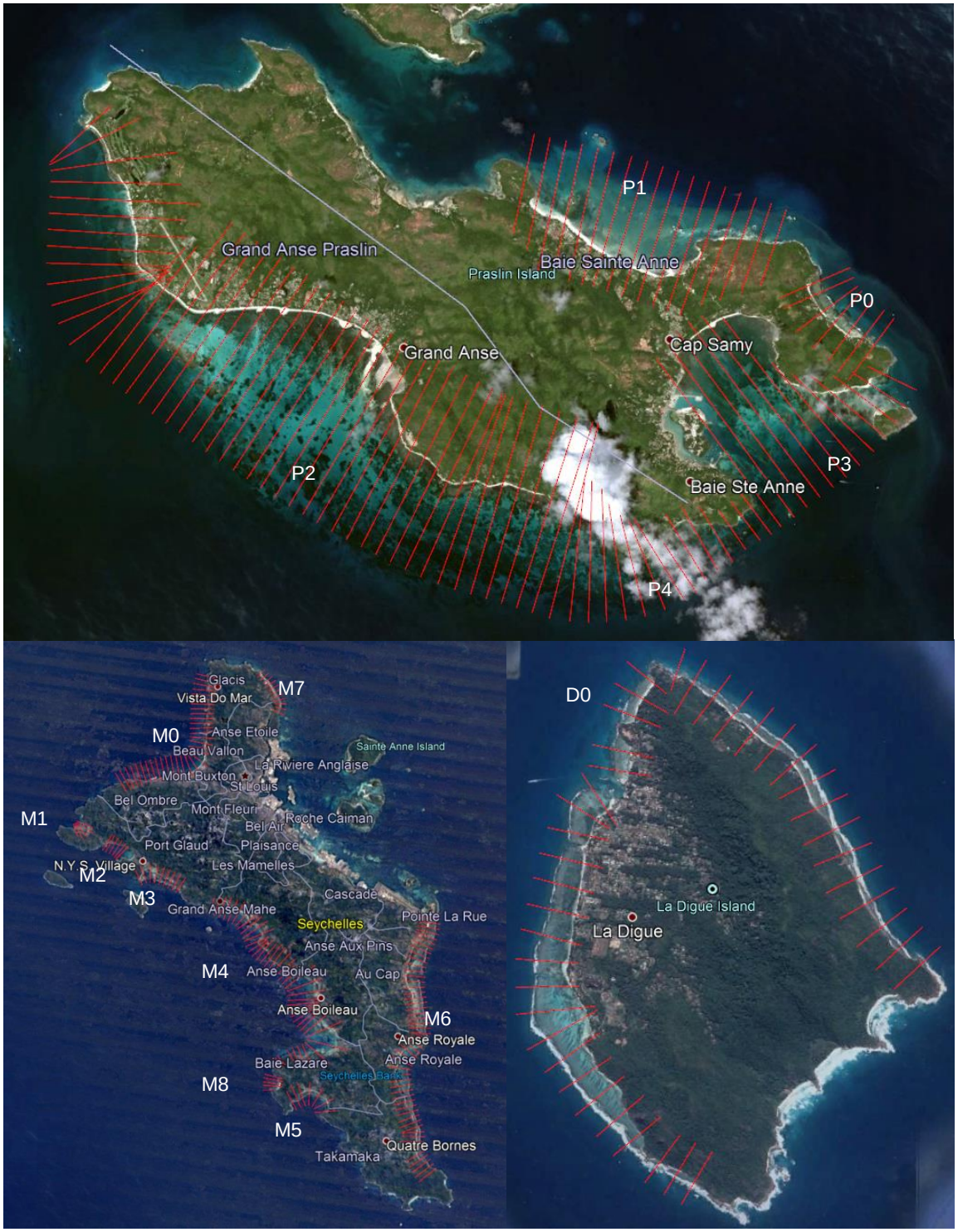

Figure 4.1 Defined transects for analysis of reef width, coral cover, and shoreline position plotted in red. The naming of different coastal stretches is indicated in white. Scale differs between islands. The island of Praslin is shown at the top, Mahé is shown on the bottom left and La Digue on the bottom right.

4.2 Reef widths

The reef widths are obtained based on the shoreline position and the position of wave breaking per transect.

The shoreline position is found based on the histogram of all NDWI pixels in the image. An unsupervised classification method is used to separate NDWI values indicating water from NDWI values indicating land. A single separation threshold is used per image. The position of separation between land and water pixels results in a shoreline position per transect. Figure 4.2 shows example signals along two transects. The shoreline position is indicated using a yellow dot. For all transects, the shoreline position is around a steep gradient in NIR reflectance, with fluctuating, consistent NIR values on the landward side and a flatter signal on the seaward side over the images. This indicates that the shoreline position is indeed a transition between land and water.

To obtain the location of wave breaking, the NIR signal over the transect based on 7 recent and high-quality satellite images is used. Wave breaking results in a distinct peak in each of the 7 images, which is automatically detected using a peak detection algorithm. First, the NIR peaks on the seaward extent of the transect (based on the shoreline position) are detected for each satellite image (indicated with crosses in Figure 4.2). A weighted mean peak location is then calculated based on the 7 peak locations (mean breaker line, indicated as a red dot). The weight of each peak is based on the reflectance value of each peak. As a reference, the average NIR signal is also calculated and used to detect a single peak (i.e. average breaker line, indicated as a green dot). In case the mean and average breaker lines show a large offset, the transect is flagged for visual inspection.

In the case of transect *La Digue_D0_28*, wave breaking is detected at the NIR peaks, and a mean breaker line (red dot) is found. In combination with the shoreline (yellow dot), this results in a reef width of 222 meters. In case of transect *Praslin_P2_23*, a flat NIR signal is found, indicating the absence of wave-induced foam. Therefore, in this case an uncertain breaker line is found in this case. Based on visual inspection of the NIR signal these transects are marked with a quality flag. Section 5 provides more information on how this quality flag is treated.

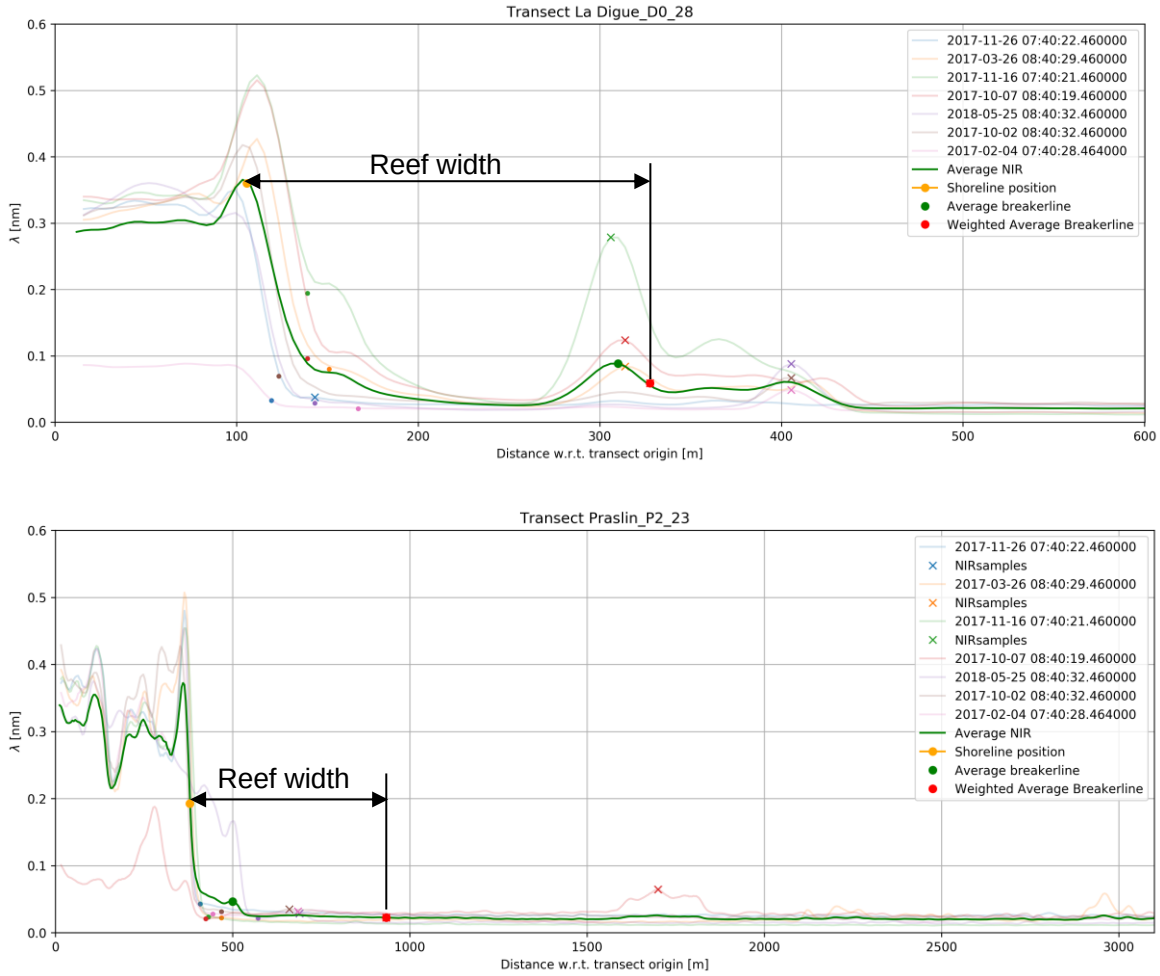

Figure 4.2 NIR information of 7 Sentinel 2 images for transect La Digue_D0_28 (top) and transect Praslin_P2_23 (bottom). Based on an automated peak detection method the breaker line is found for each Sentinel 2 image in order to obtain an mean breaker line.

A spatial overview of the resulting shorelines, breaker lines and beach widths per coastal site are presented in Figure 4.3 (La Digue), Figure 4.4 (Praslin) and Figure 4.8 (Mahé).

For La Digue, most detected shorelines and breaker lines follow the reef geometry. However, on the eastern end of the island, the reef becomes narrow, and detection becomes challenging due to the satellite image pixel resolution. These transects are flagged. On the east coast of La Digue, more gently sloped beaches are found rather than the characteristic fringing reef geometry with a steep fore reef, a sharp break in slope at the crest, and broad reef flat (e.g. Figure 3.1).

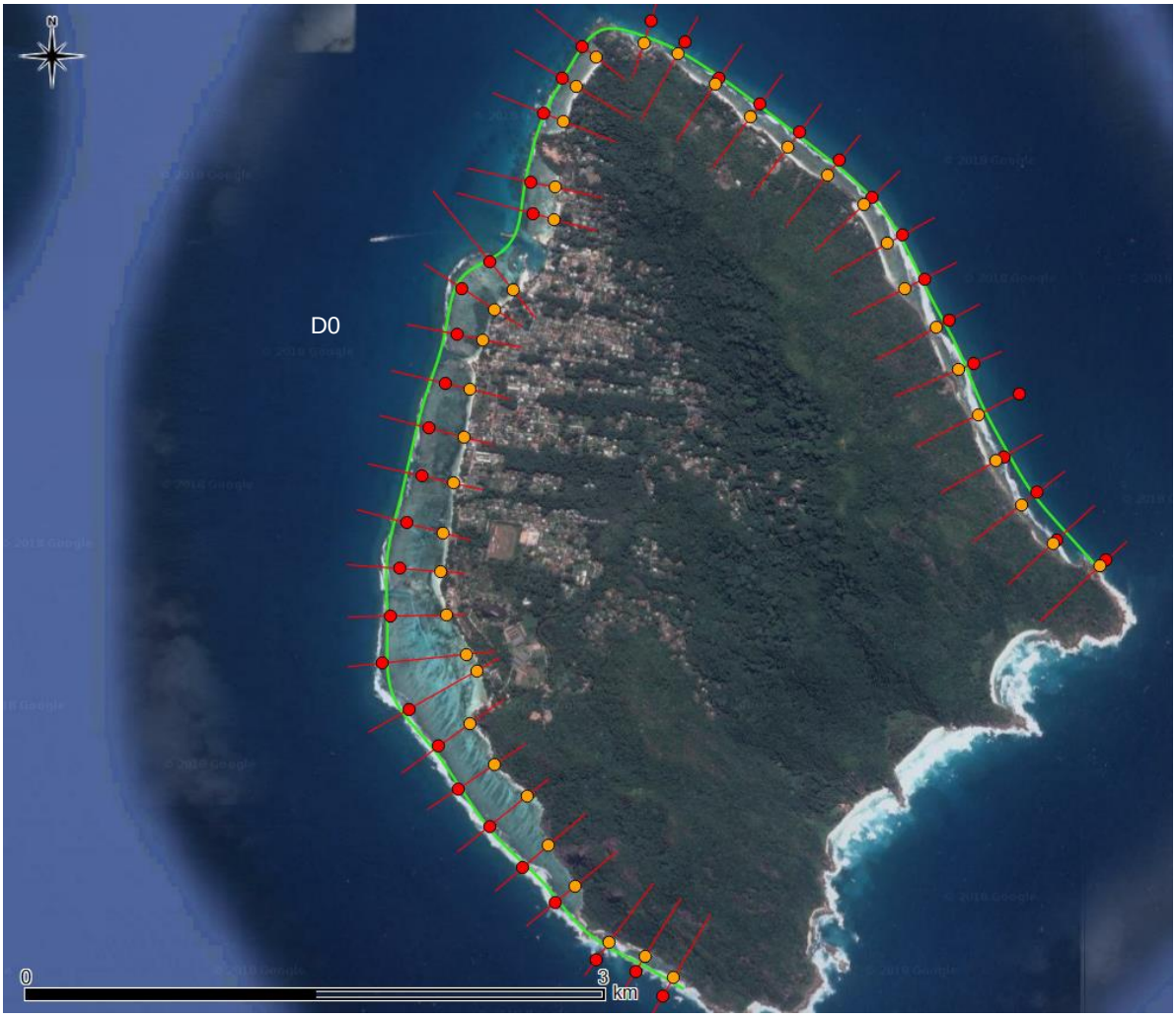

Figure 4.3 Shoreline positions (orange dots), mean breaker line positions (red dots), transects (red) and alongshore spline (green) for the island of La Digue.

For Praslin, sites P0, P2 (west) and P4 show typical fringing reef geometries, consistent with Figure 3.1, and hence a breaker line that is consistent with visual inspection. For sites P1, P2 (east) and P3, a fringing reef geometry seems absent and hence no wave breaking is present. Alternatively, wave breaking happens at various locations along the transect (depending on wave conditions and image time acquisition). This results in scattered breaker line positions and less accurate reef widths.

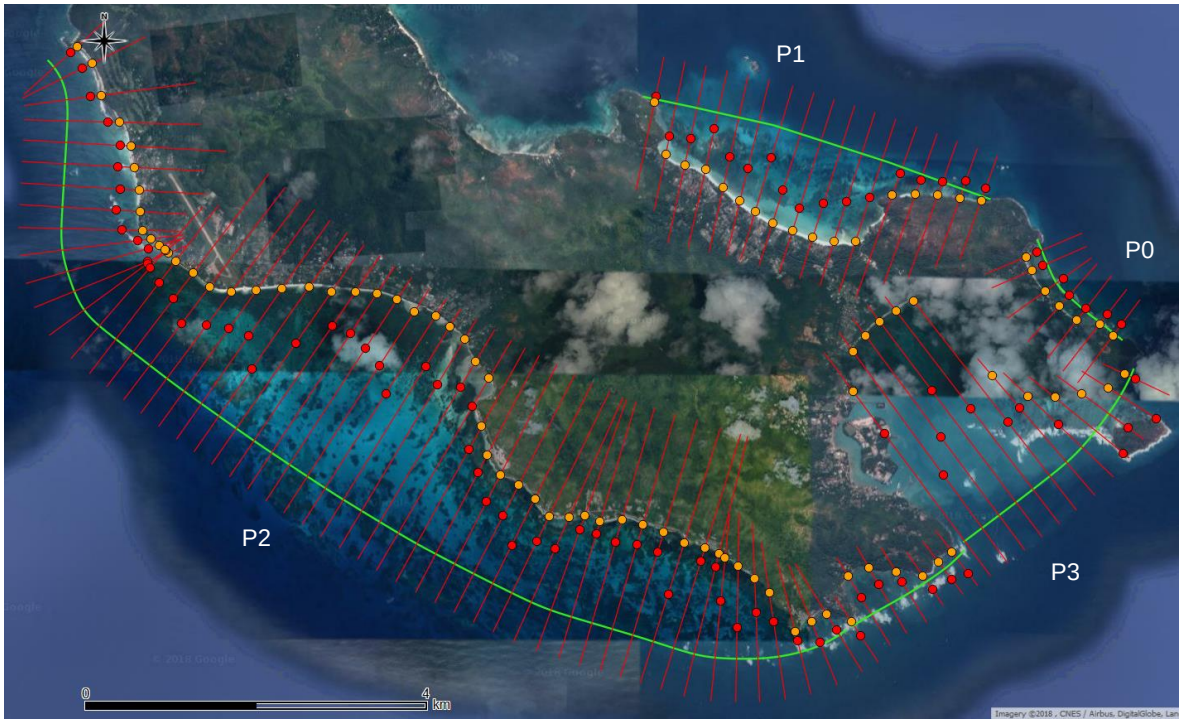

Figure 4.4 Shoreline positions (orange dots), mean breaker line positions (red dots), transects (red) and alongshore spline (green) for the island of Praslin.

For Mahé, good detection of breaker lines and shorelines is found at the sites M3, M6 and M7, since wave breaking results in a distinct NIR signal at most transects. The transects at site M0 show less distinct wave breaking on all Sentinel images, but still a consistent breaker line is obtained at the northern end of the coastal stretch. Sites M4 and M8 show varying breaker line positions along the transects, indicating the absence of a sharp reef crest. Although sites M1 and M2 comprise embayed beaches and hence show less distinct wave breaking, a consistent breaker line is still found. M5 is also embayed, but with fewer wave breakers and therefore an uncertain breaker line.

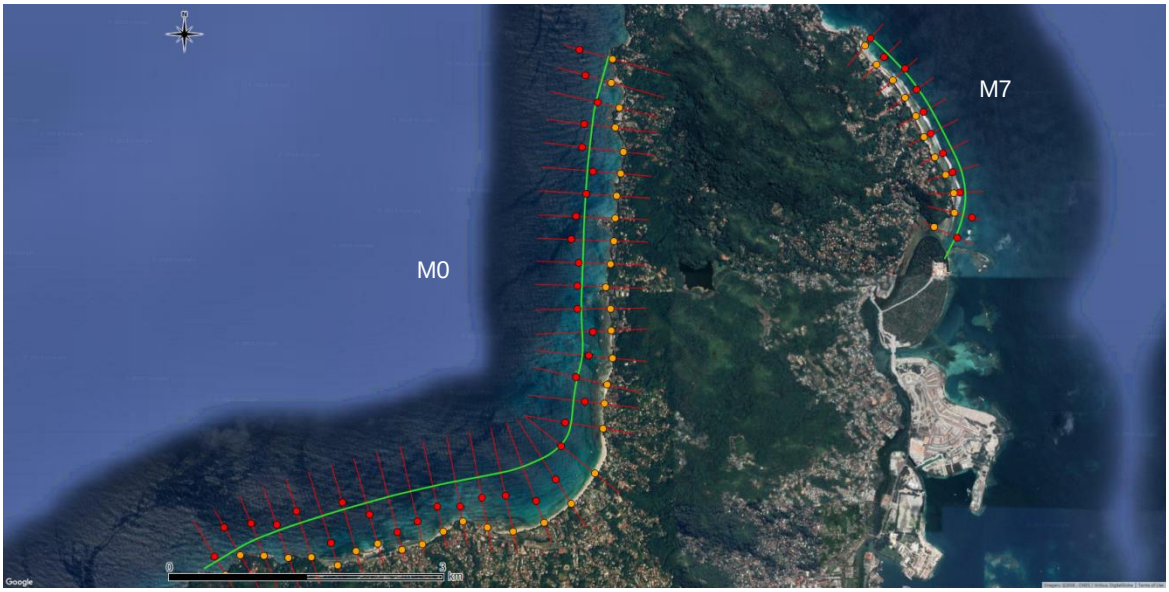

Figure 4.5 Shoreline positions (orange dots), mean breaker line positions (red dots), transects (red) and alongshore spline (green) for the island of Mahé (sections M0 and M7).

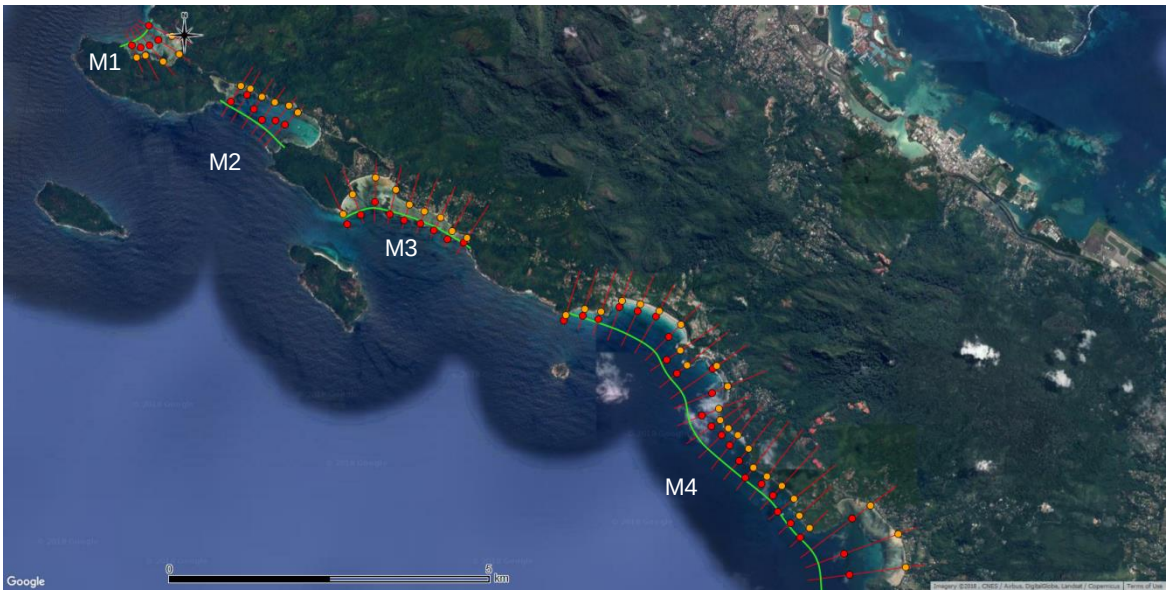

Figure 4.6 Shoreline positions (orange dots), mean breaker line positions (red dots), transects (red) and alongshore spline (green) for the island of Mahé (sections M1 to M4).

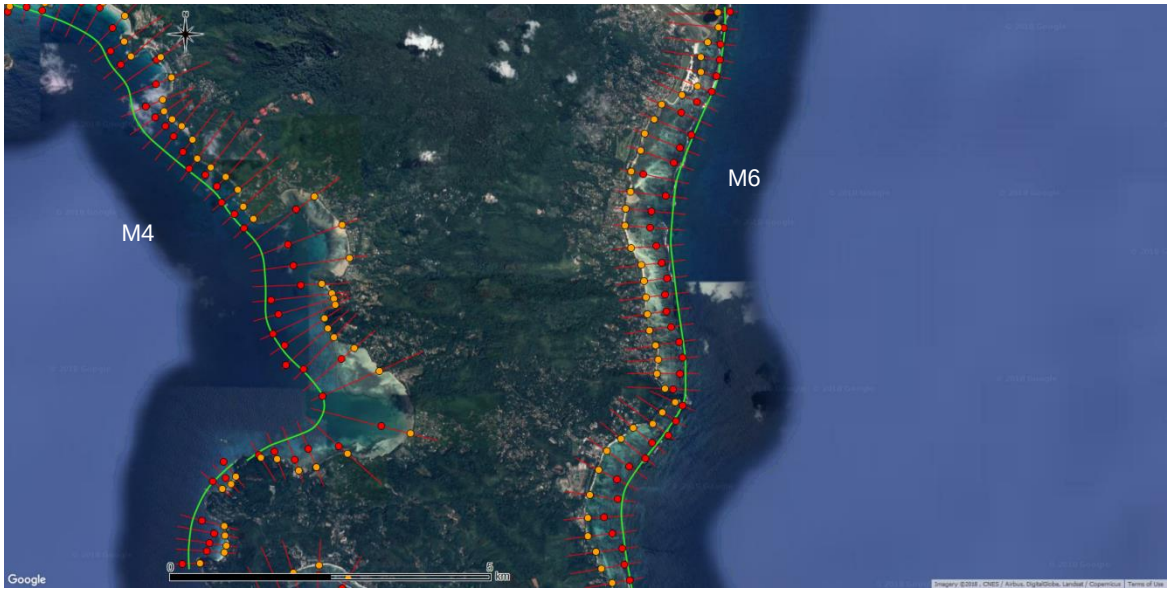

Figure 4.7 Shoreline positions (orange dots), mean breakerline positions (red dots), transects (red) and alongshore spline (green) for the island of Mahé (sections M4 and M6).

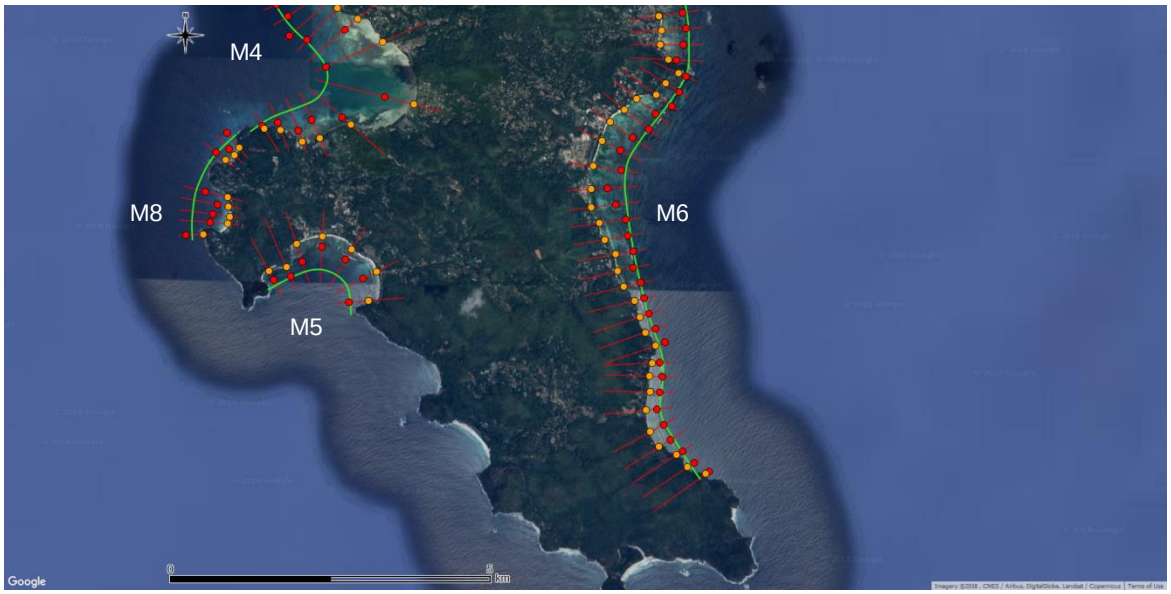

Figure 4.8 Shoreline positions (orange dots), mean breaker line positions (red dots), transects (red) and alongshore spline (green) for the island of Mahé (sections M4, M8, M5, and M6).

All NIR and elevation outputs are manually checked for quality based on the presence of a wave breaking peak (indicating the reef break) and/or the estimation of an uncertain fore reef slope. For 31% (96 out of 308) of the transects, no clear wave breaking peak was found, which suggests that these profiles do not conform to the idealized fringing reef profiles for which our method is developed (and schematized in Figure 3.1). However, a reef width is still provided based on the best estimate of the position of wave breaking. For those transects where the method finds unrealistically mild slopes, the fore reef slope is restricted to a value of 1/50. These are marked with a quality flag based on visual inspection (
Figure 4.9 to Figure 4.11), which can later be used to assess confidence in the runup reduction results for a given transect. For instance, La Digue has 8 transects with uncertain fore reef slopes and no transects with uncertain reef widths (Figure 4.9). Transects with high confidence are not displayed in this figure.

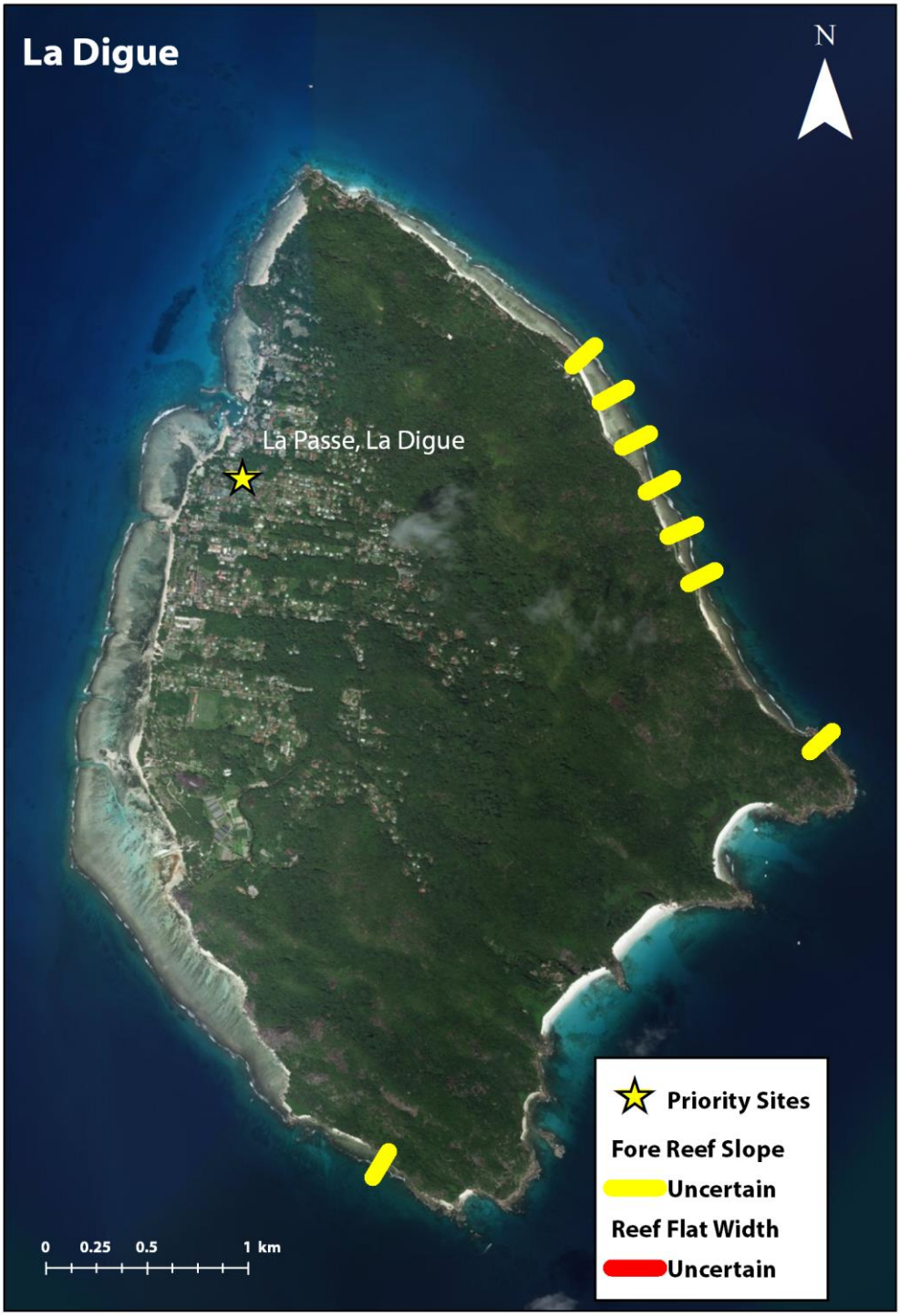

Figure 4.9 Quality control flags for La Digue. Flags indicate transects where the method found very mild fore reef slopes (yellow) or was uncertain about reef widths (red).

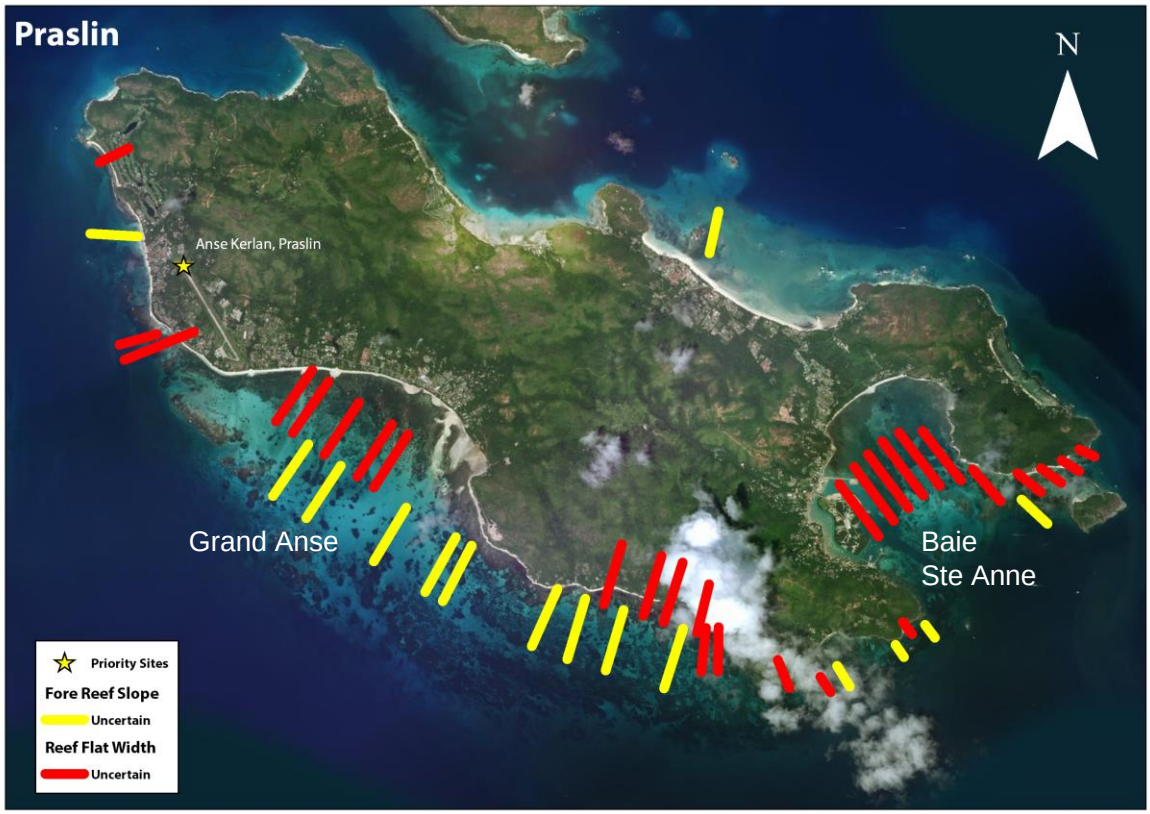

Figure 4.10 Quality control flags for Praslin. Flags indicate transects where the method found very mild fore reef slopes (yellow) or was uncertain about reef widths (red).

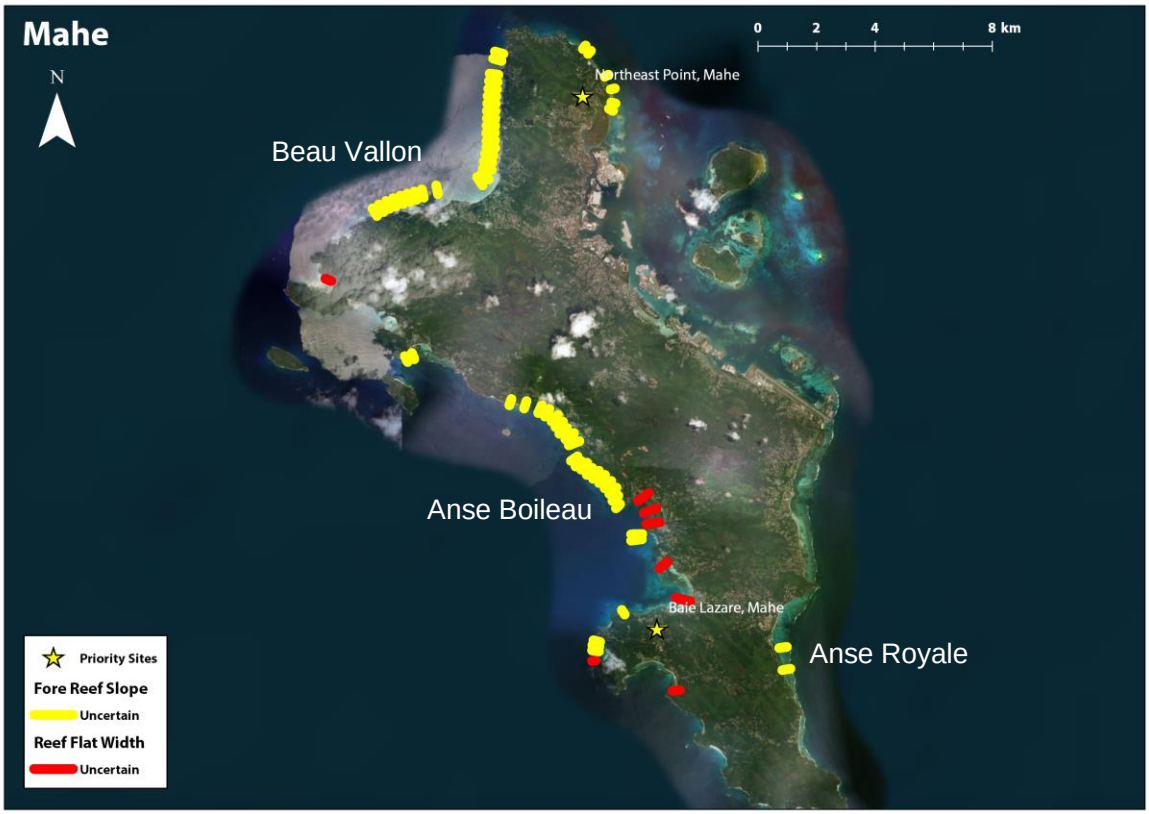

Figure 4.11 Quality control flags for Mahé. Flags indicate transects where the method found very mild fore reef slopes (yellow) or was uncertain about reef widths (red).

For La Digue (
Figure *4.9*), all of the transects had well-defined reef widths, and only a few were estimated to have uncertain slopes (yellow bars). Praslin had considerably more uncertainty, particularly along the southwest coast and in Baie Ste Anne for reef width red bars) and for reef slope on the south-west coast (yellow bars) (
Figure *4.10*). The reef widths of Mahe were easily defined on most transects, such as at Anse Royale, which has a typical fringing reef geometry. The only notable exceptions are several transects within Anse Boileau (Figure 4.11). Beau Vallon's and Anse Boileau's fore reef slopes were uncertain as well. The potential runup reduction calculated for these sections should be regarded with caution.

4.3 Beach slopes

The beach slopes are derived from the Digital Terrain Model (DTM) as provided by the client along the transects as described in the previous chapter. The transects were split at the shoreline points, as only the landward side of the transect is accounted for in the beach slope analysis (orange dots in Figure 4.3 to Figure 4.8). The elevation from the DTM is then extracted using ArcGIS (Figure 4.12).

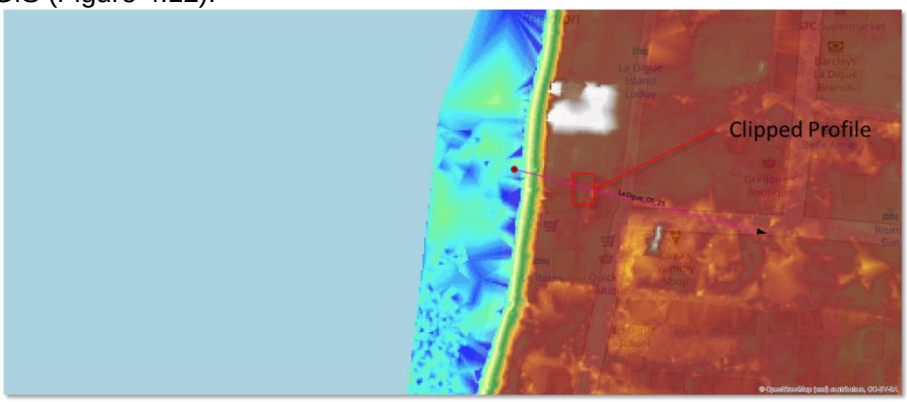

Figure 4.12 Example of transect in La Digue. It shows the landward section (clipped at the shoreline) with the underlying Digital Terrain Model (DTM).

The slope is calculated using a moving average with a range of 13 cells (i.e. 6 meters before and 6 meters after the point under consideration), as demonstrated in Figure 4.13. Using the maximum slope determined by the 13 point method gave stable estimates when compared to other approaches (e.g. 7 points). The method was applied in the same way to the DTM data of Mahé and Praslin. A small number of profiles is identified which does not give accurate results and will therefore be excluded in the runup analysis.

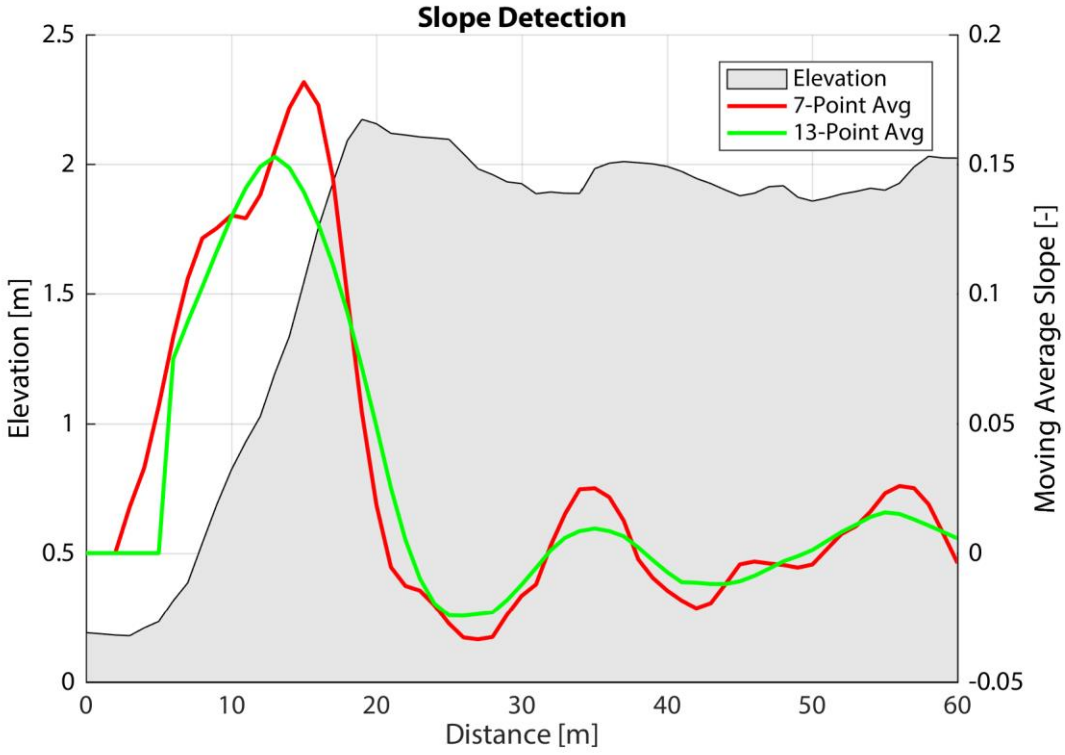

Figure 4.13 Visualisation of the slope values for 7 cells (red) and 13 cells (green).

4.4 Hydrodynamic forcing

The hydrodynamic forcing obtained from the literature which was presented in section 3.5 was used in the computations. The wave forcing applied to each segment of the islands is shown in Figure 4.14. The scarcity of data is evident here, as in reality the wave forcing will show more alongshore variation due to prevailing wind directions, propagation of wave fields, etc. In order to compute more accurate and site-specific wave fields, a wave climate study should be performed, which is outside the scope of this study.

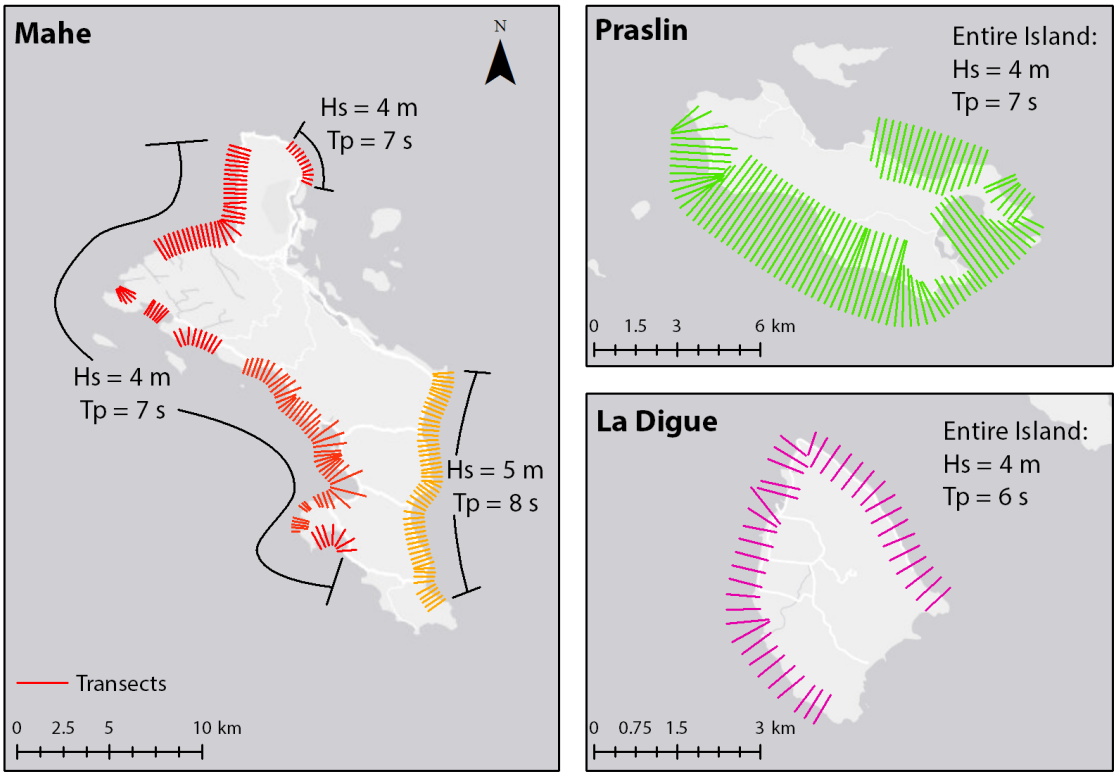

Figure 4.14 Applied wave boundary conditions along the islands' shores. Mahé (left), Praslin (top right), La Digue (bottom right).

4.5 Reef elevation

The reef elevation per transect is obtained using a single, cloud-free Landsat 8 image per coastal site. The shoreline position in combination with the tidal water level that was present during satellite image acquisition is used to reference the elevation with respect to MSL Based on the elevation along the transect, the average reef depth and the offshore slope are obtained. Figure 4.15 shows the elevations for two example transects (the same transects as in the section about reef widths). For transect *La Digue_D0_28* a clear breaker line was present and hence a distinct fringing reef geometry was obtained. For transect *Praslin_P2_23,* breaking was absent, and the resulting topography shows a less distinct fringing reef geometry.

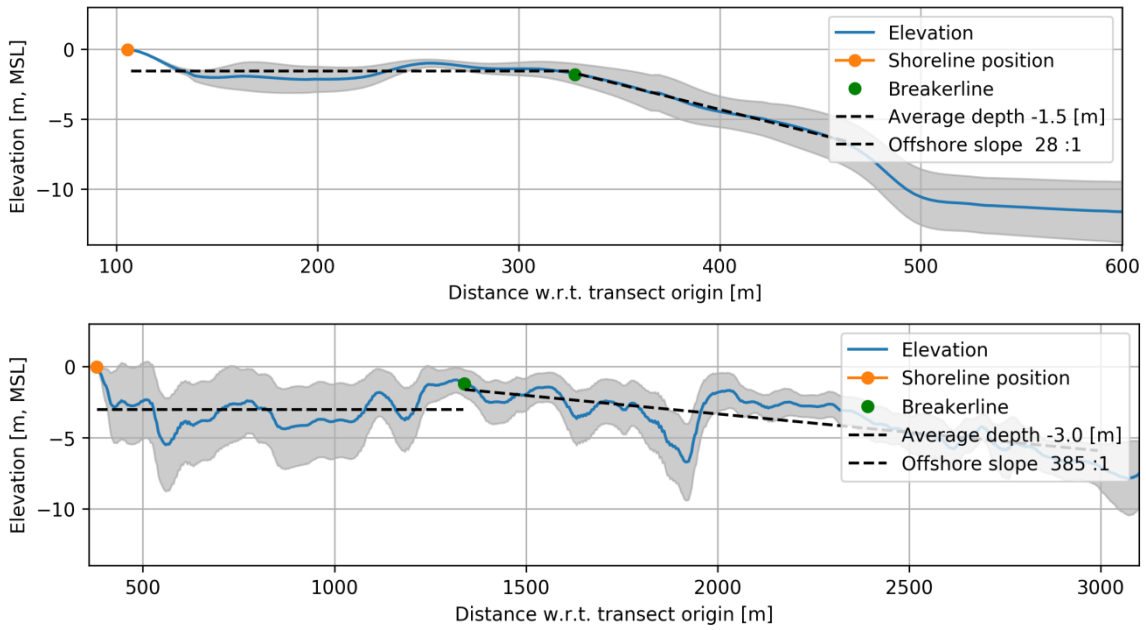

Figure 4.15 Elevation obtained from a Landsat 8 image for transect La Digue_D0_28 (top) and transect Praslin_P2_23 (bottom). The obtained shoreline and breaker line positions (as described in section Reef widths) are indicated with dots. The uncertainty estimate based on the range of calibration values is indicated in grey. The average depth and offshore slope are indicated as a dotted line.

To provide a ground truth for the estimated reef widths and slope, several checks were conducted using surveyed bathymetric charts provided by the client. The charts required labour-intensive digitization which was beyond the scope of the present quick-scan project, so only a limited number of locations were examined. Based on the analysis in Figure 4.15, a mean reef width of 222 m, reef depth of 1.5 m, and fore reef slope of 1/28 were estimated for transect *La Digue_D0_28*. When this schematized reef is overlaid on the measured bathymetry, there is a reasonable qualitative fit along the reef flat and upper fore reef, given that the schematization allows for only one horizontal reef flat segment and a single foreshore slope.

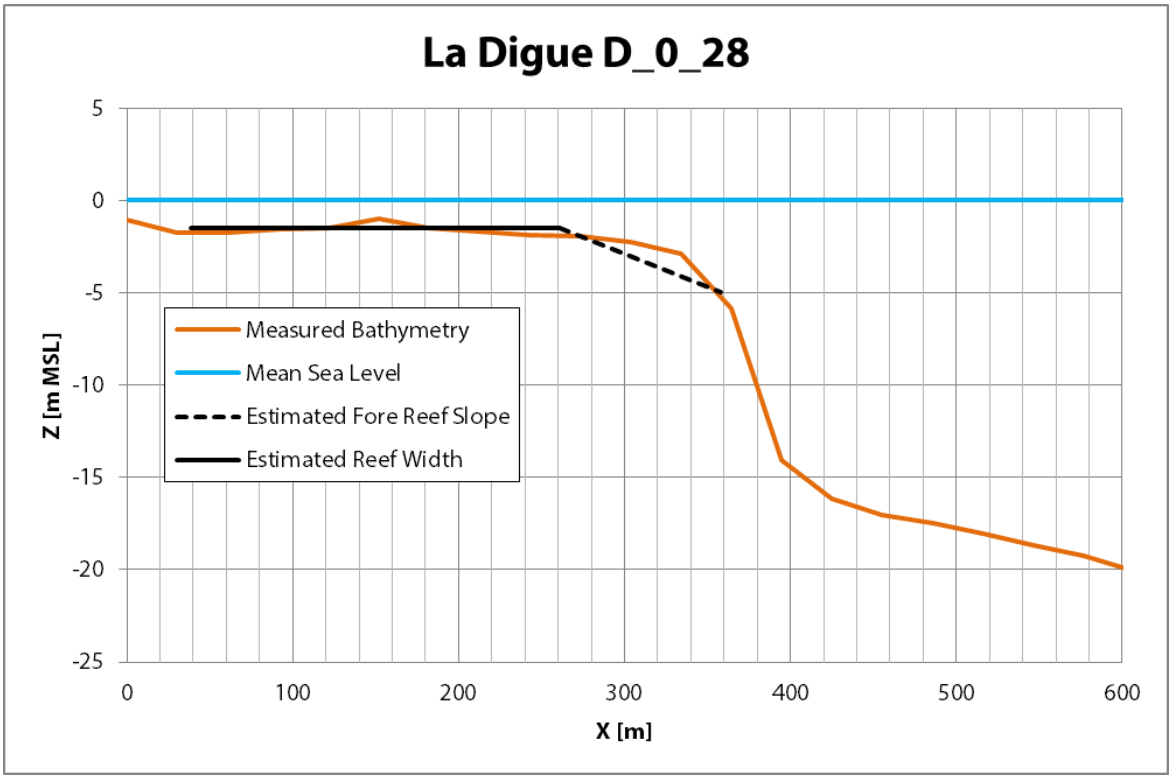

Figure 4.16 Comparison of surveyed bathymetry and schematized reef geometry based on remote sensing analysis for La Digue D0_28.

A similar comparison was done at transect *Mahé_M1_1*. The remote sensing analysis yielded a mean reef width of 398 m, reef depth of 0.8 m, and fore reef slope of 1/56. Visual inspection of the transects in Figure 4.17 also finds a reasonable approximation of the reef flat and upper fore reef slope.

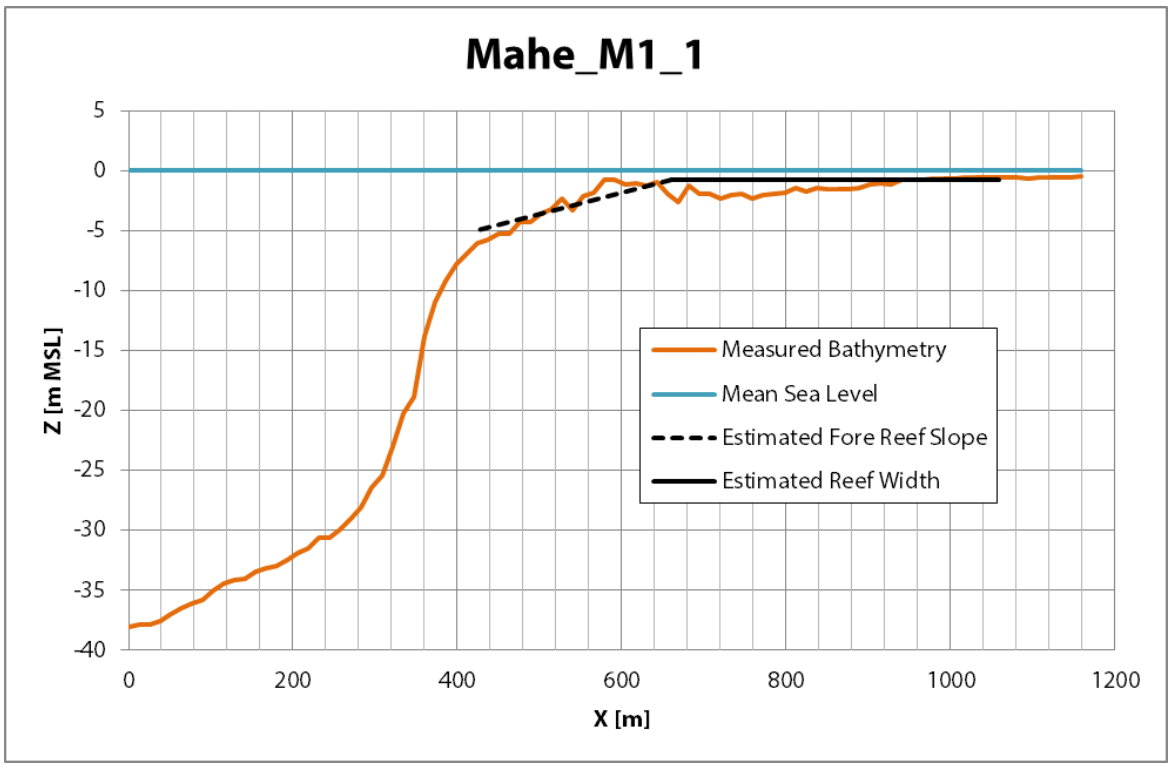

Figure 4.17 Comparison of surveyed bathymetry and schematized reef geometry based on remote sensing analysis for Mahé_M1_1.

The mildest fore reef slope in the BEWARE system is 1/50, so milder slopes measured through remote sensing were limited at that value. However, this yields a conservative estimate for wave runup, since runup is greater for steeper fore reefs (Pearson et al., 2017a). On La Digue (
Figure 4.9), the only flagged transects were along the east coast of the island. On Praslin, many of the transects along the southwest coast were also flagged (Figure 4.10). These reefs had extremely mild, curving slopes that bore minimal resemblance to the schematized fringing reef profiles used in the BEWARE system. Hence, this area merits further investigation with a more detailed numerical model. Mahe also had several stretches of coastline with very mild fore reef slopes, along Baie Beau Vallon, Grand Anse, and North East Point (Figure 4.11). These locations should also be investigated further with more detailed measurements and models.

4.6 Reef rugosity

The current reef state is studied through a literature survey, which is summarized in 4.6.1. Quantitative data on structural complexity is very scarce, as is detailed data of past and present coral coverage. This study will not present an assumed coral coverage map of the transects under consideration. Rather, the sensitivity of the model to a range of roughness coefficients, representing the relative degrees of coral coverage, is examined in a range of cf = 0.001 (sandy beach with no coral cover), cf = 0.01 (low coral cover and roughness), cf = 0.05 (medium roughness) to cf = 0.1 (high coral coverage with complex structures). We refer to Section 3.7 for the justification of the selected values.

4.6.1 Literature study on the state of coral reefs in the Seychelles

The 1998 bleaching event at the coral reefs of the Seychelles induced a sequence of studies on the health and recovery of coral reefs at and around the Seychelles. A Seychelles wide average of 80-90% mortality of corals was observed based on coverage percentages (Goreau 1998). Lag effects in the mortality after the bleaching event can be identified in the decreasing size structure of the fish communities at the remaining coral reefs (Graham et al., 2007).

Coral coverage and the health of the present corals is reported upon in the period 1994-2011 in Wilson et al. (2012) at seven regions around the Seychelles. In 2011, only 14% of study sites were covered with corals, only half of the coverage present before the major bleaching event. Where algae cover had increased, since bleaching, no recovery of the coral reefs has occurred.

On 26 December 2004, the Boxing Day Tsunami hit the Seychelles. Abdulla et al. (2006) reported on the damage (decrease in coverage percentages) on the coral reefs as a consequence of the tsunami, concluding that only reefs in the direct impact line of the tsunami were significantly affected. Damage to carbonate reefs was generally larger than on granite reefs, which could be attributed to the larger amount of coral rubble that was typically present on carbonate reefs.

Natural recovery of coral reefs after such a large bleaching event is difficult, as young corals are much more vulnerable to stress events than fully developed reefs (Chong-Seng et al. 2014). At some locations, corals are completely displaced by algae. Graham et al. (2006, 2015) observed regime shifts in 9 out of 21 studied coral reefs in the Seychelles from coral dominated to algae-dominated.

4.7 XBeach computations

The observed reef fore reef slopes, beach slopes, reef widths, reef depths, and the hydrodynamic boundary conditions described in the above paragraphs provide a parameter range for the associated runup to be computed. In the absence of sufficient measurements of reef hydrodynamics, the BEWARE Bayesian network uses a synthetic dataset derived using a process-based numerical model. More details can be found in Pearson et al. (2017).

The hydrodynamic forcing and reef geometry of the transects used in this project exceeded the parameter space of the original BEWARE database. As such, the database was expanded using the non-hydrostatic XBeach model (Roelvink et al., 2009, 2017). Figure 4.18 shows histograms of the distribution of the XBeach computations over the bin-choice of the independent variables in the BN. Each unique permutation of the bins in the histograms formed the basis of a set of XBeach computation. In combination with the existing database, this resulted in a total of ~60,000 XBeach computations.

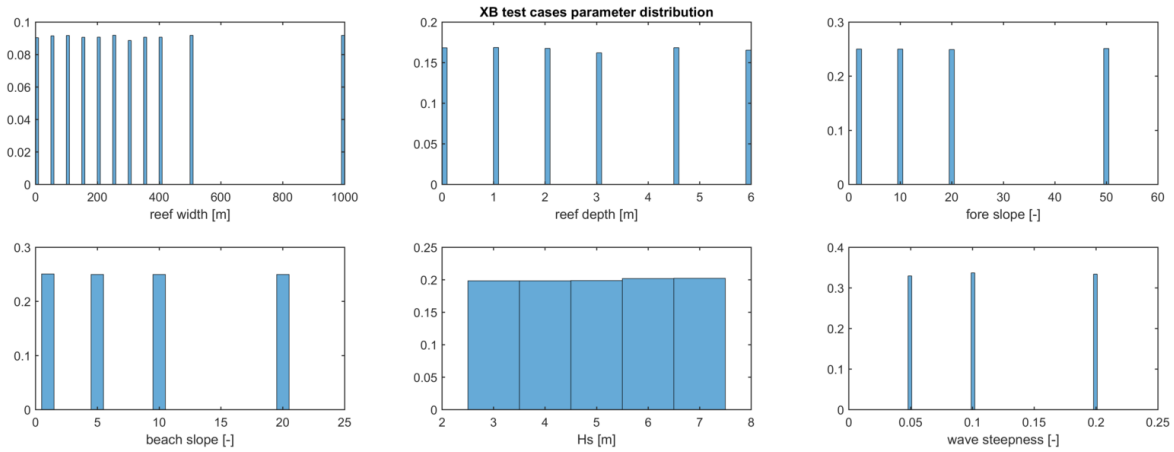

Figure 4.18 Distribution of XBeach computations over the parameter space of the Bayesian Network

The 2-hour simulations are further separated into four 30 min simulation periods with random realizations of the surface elevation time series at the offshore boundary. This gives runup time series, where runup is defined as the highest vertical level at the beach which becomes wet. $R_{2\%}$ is defined as the vertical level which is exceeded 2% of the time. The complete set of hydrodynamic forcing, geometric reef properties, and runup results yielded approximately ~250,000 unique training cases for the Bayesian Network (BN).

Note that the peak wave period associated with waves of a certain significant wave height is captured in the BN through the variable wave steepness (Hs/L). The wave length (L) follows from the wave period through the dispersion relationship, to ensure that the offshore wave conditions remained physical for each of the parameter combinations.

Figure 4.19 shows four example XBeach profiles from the training dataset. The offshore water depth in the profiles is based on a deep water criterion for the wave number ($k \cdot h = 1$). This means that the offshore boundary for wave conditions with a larger (smaller) wave number lies shallower (deeper). The beach is extended to 30 meters of height such that the recordable run-up range is 30 m as well, in effect an infinite slope. This enables easier intercomparison between different profiles, since hinterland elevation does not need to be computed for each case: instead, runup is used as a proxy for overwash and flood potential. The grid resolution is dynamic over the transect such that local wave length is resolved and Courant number remains as constant as possible over the domain, with a minimum grid resolution of 0.25 m.

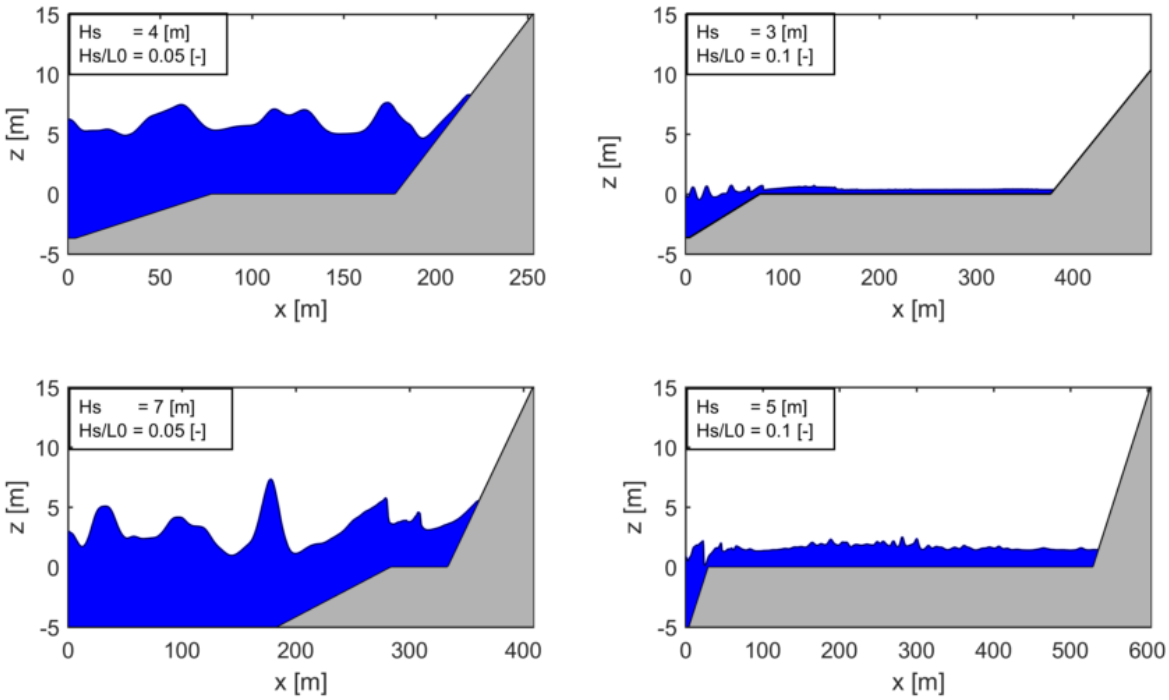

Figure 4.19 Four examples of XBeach profiles from the training dataset with the instantaneous water level superimposed. In each profile, the wave height (Hs), wave steepness (H0/L0), and reef geometry vary.

4.8 Bayesian Network construction and training

The cases from the XBeach computations are used to train a Bayesian Nework, which can be visualized as in Figure 4.20. This network shows probability distributions for all input and output variables across the entire data set. Input parameters were discretized using the same parameter values as were tested in XBNH, resulting in uniform distributions. This trained network can be queried for a particular set of reef parameters belonging to a given transect. By further constraining for a particular water level, wave height, and steepness, the estimated runup is then given as a probability distribution.

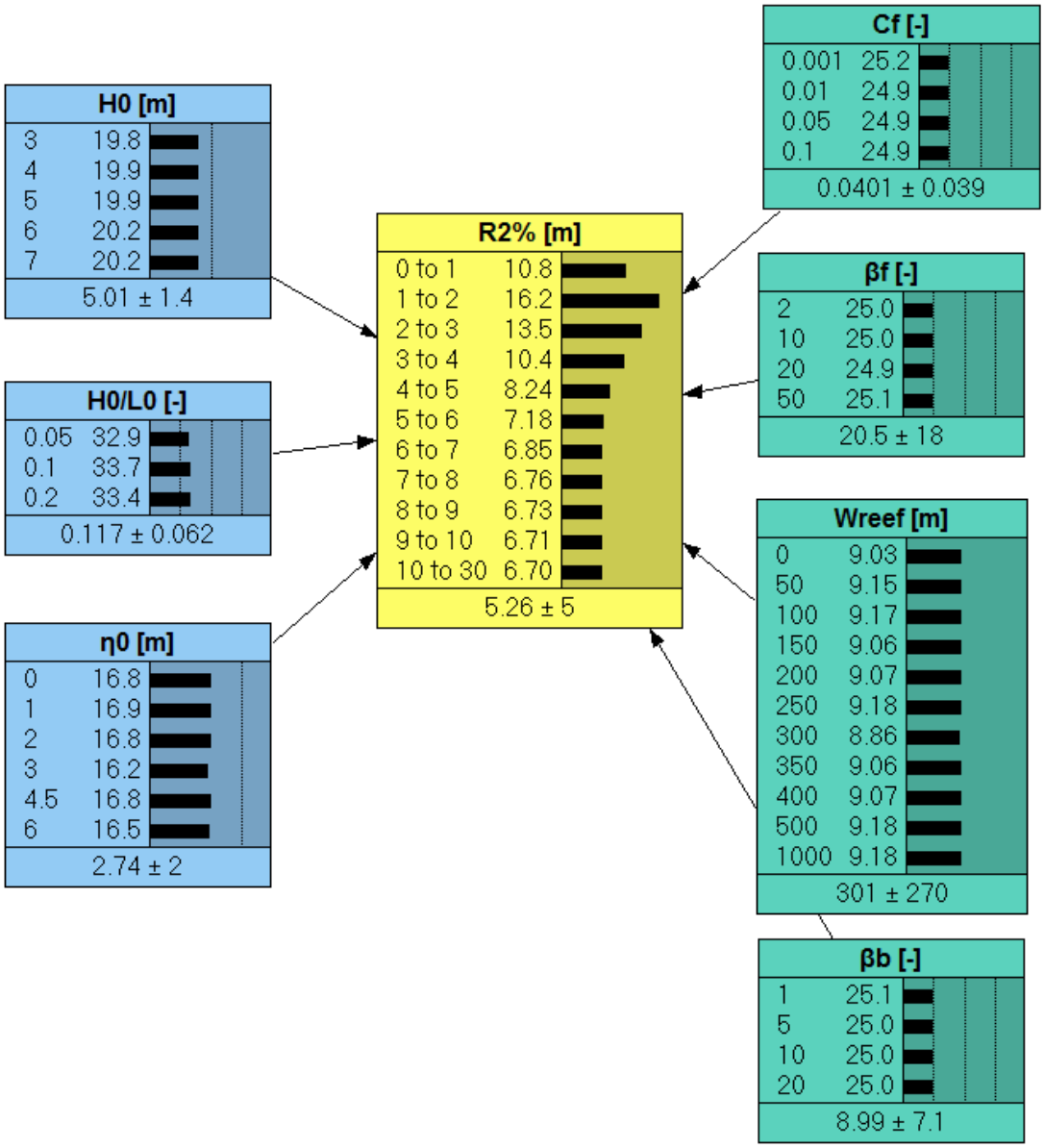

Figure 4.20 Example of Bayesian Network relating hydrodynamic forcing (H0 Wave height, H0/L0 wave steepness, η0 water level) and reef parameters (Cf roughness, βf forereef slope, Wreef reefwidth, βb beach slope) to the resulting R2% wave runup.

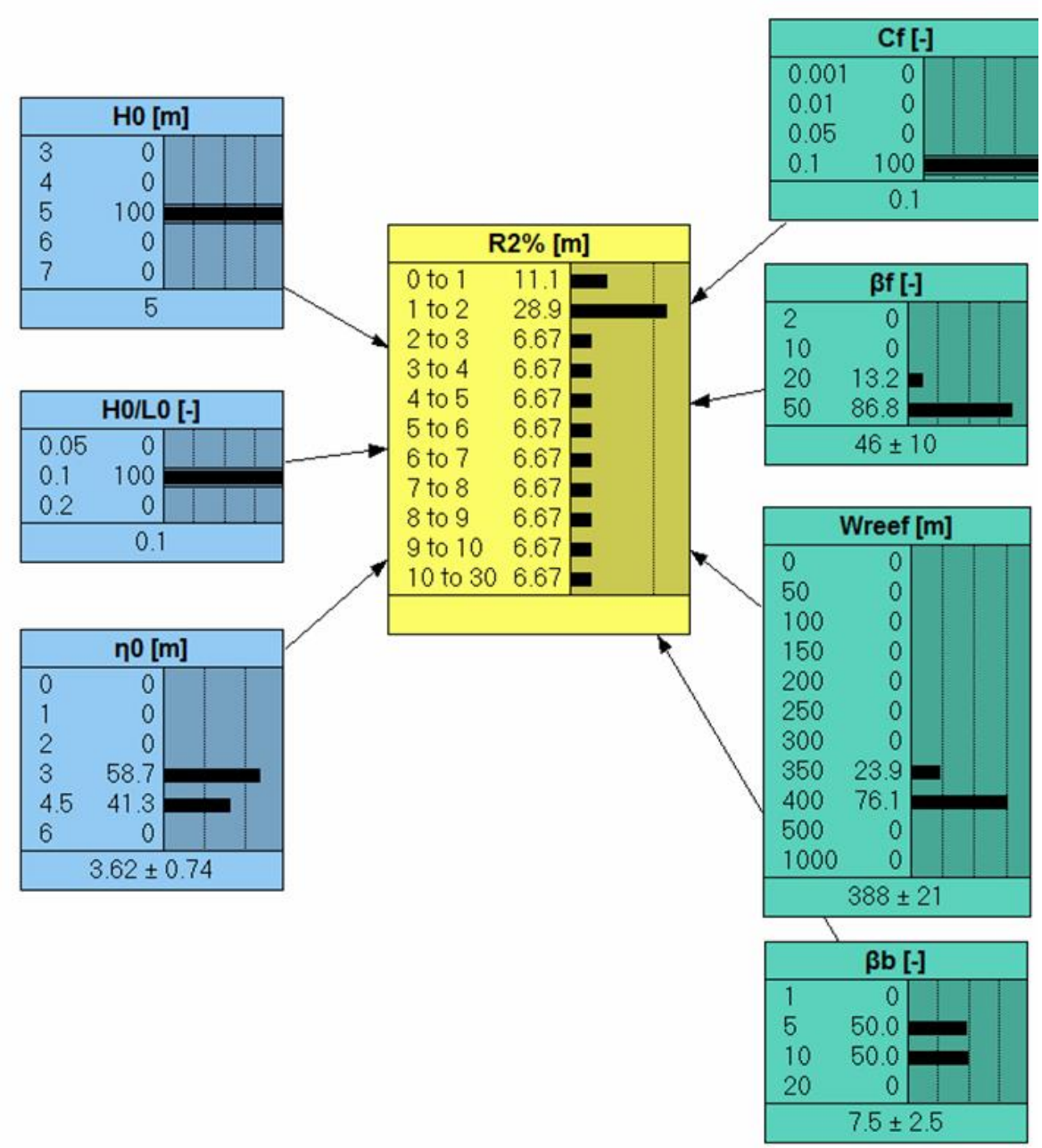

Figure 4.21 Example of Bayesian Network with constrained parameter values for the hydrodynamic forcing (H0 Wave height, H0/L0 wave steepness, η0 water level), reef parameters (Cf roughness, βf fore reef slope, Wreef reef width, βb beach slope), and the resulting $R_{2\%}$ wave runup.

For example, in Figure 4.21, we examine a hypothetical reef that is 388 m wide, has a fore reef slope of 1/46, a beach slope of 1/7.5, and a roughness coefficient of 0.1 (representing high coral cover). If it is subjected to 5 m waves with a steepness of 0.1 and water level of 3.62 m, we obtain a probability distribution for $R_{2\%}$ which indicates that a runup value between 1 and 2 meters is most likely (the mode), with a smaller chance of runup in the lower bin of 0-1 m. In order to account for the distribution over multiple bins (including in some cases a bimodal distribution), rather than using the mode, we computed the expected value of the $R_{2\%}$ runup, where we excluded the uniform background uncertainty.

5 Changes in runup as a function of reef roughness

5.1 Approach

The change in runup by varying the roughness has been visualized in a so-called “bacon strip plot”. In this way, we can visualize the effect that friction has on the runup reduction. For every transect we visualize the absolute reduction in wave runup between the case of no friction minus high friction (outer strip), no friction minus medium friction (middle strip) and no friction minus low friction (inner strip), where darker colours give a large reduction and light colours suggest that there is little difference.

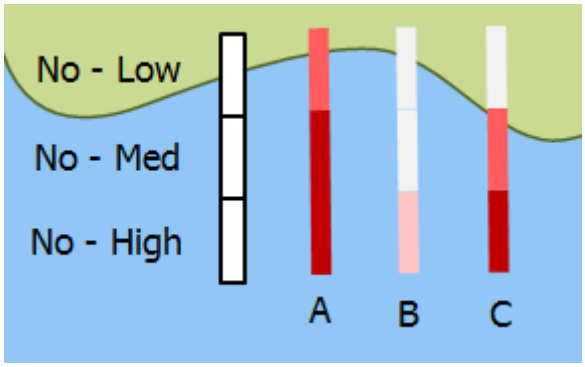

Figure 5.1 Guide to interpreting the relative runup reduction plots. The landward box represents the incremental decrease in runup as the result of moving from a no-coral state to a low coral cover state. Similarly, the middle box depicts the incremental decrease in runup as the result of moving from a no-coral state to a medium coral cover state. The seaward box indicates the maximum possible runup reduction, as the result of moving from a no-coral state to one with high structural complexity.

This absolute reduction is graphically represented as in Figure 5.1 with red sections of coastline indicating an increased reduction of runup. Along the coastline of all three islands, the absolute reduction in runup will thus indicate areas in which an incremental increase in hydrodynamic roughness (e.g. coral reef restoration) will have an effect on the runup.

These plots can be used in two ways. First, to identify the sites where reef restoration would have the most potential benefit, examine the overall colour of each transect. The *areas* where colours are darkest indicate those with the greatest runup reduction. For instance, areas with a small existing reef widths are expected to afford little runup reduction irrespective of roughness, while waves will have more time to be attenuated by friction on a wider reef.

The second way to use these plots is to compare the *level* of roughness that produces the largest reduction, i.e. by examining the colour changes along a transect. For a potential site, this gives information about the degree of increased roughness that is necessary to yield a reduction in runup. This should be compared with the present state of the reef roughness based on detailed coral cover maps, which is beyond the scope of our study.

To illustrate how to interpret the runup reduction plot, we provide three examples in Figure 5.1:

A: Increasing roughness strongly reduces runup (higher restoration potential)
B: Increasing roughness has little effect on runup (low restoration potential)
C: Profile is highly sensitive to changes in roughness; little effect for small increases but strong reduction for high roughness (restoration only effective if high roughness is achieved)

These results may then be used as guidance for reef restoration efforts. In the digital dataset we also provide plots of relative reduction where the absolute difference in runup is normalized by the runup found for the no-roughness cases. These plots are not shown in the report as they lead to the same interpretation.

5.2 Spatial Variations in Runup Reduction: Base Case 2010

First we consider the “Base Case” which are the wave and water level scenario for the year 2010, as specified in Table 3.1 and Table 3.2.
The absolute runup reduction for this case for four reef roughnesses for La Digue is given in Figure 5.2. Generally, darker colors are visible on the west side of the island, due to the wider reefs. Reefs on the east side of the island are narrower, so changes in friction have little effect on wave runup reduction, hence the generally lighter colours found there.

When considering the island as a whole, increasing from no coral cover to low coral cover has little to no effect (evident in white colour of landward band). Reefs on the west side show a strong gradient in runup reduction. Medium cover has some effect, but high cover is most effective. Conversely, medium cover has little improvement relative to no or low cover on the east side (due to the narrower reef).

The highest potential runup reduction for La Digue is at priority area La Passe, and also at Anse Union on the southwest side.

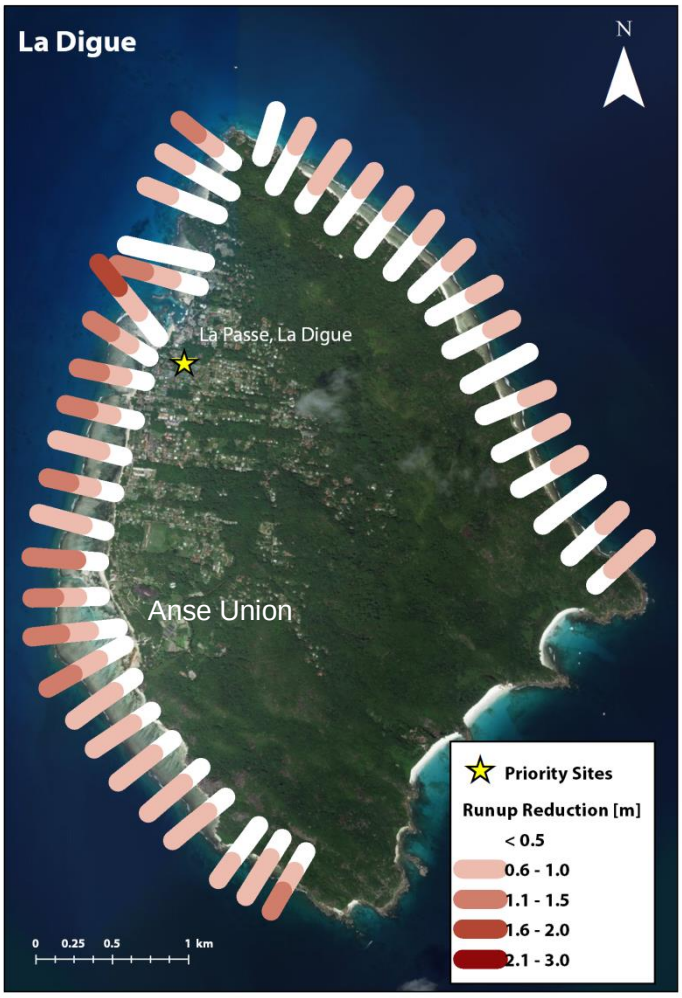

Figure 5.2 Runup reduction as a function of roughness for La Digue (2010, base case wave conditions).

The absolute runup reduction for Mahe is given in Figure 5.3. The highest potential runup reduction for the east coast of Mahe is at Anse Royale and Anse aux Pins, which are both concave bays with wider reefs. On the western side Baie Beau Vallon and Anse a la Mouche show higher potential, although Baie Beau Vallon was flagged for having very mild fore reef slopes. The potential runup reduction shows strong variability at priority sites Baie Lazare and at Anse Nord D'Est, likely due to the complex coastline and reef there. These locations should be modelled in greater detail if it is a priority for restoration.

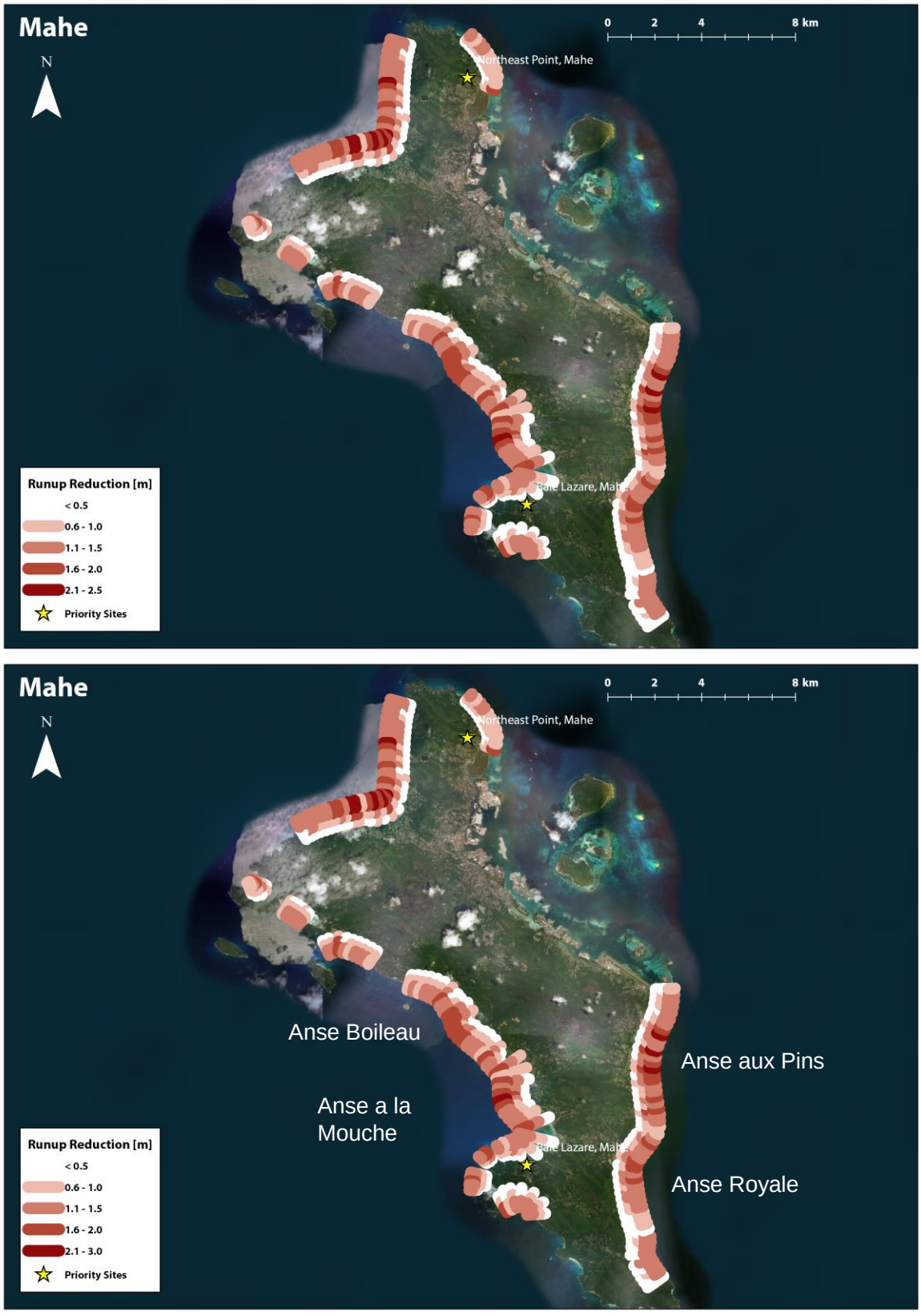

Figure 5.3 Runup reduction as a function of roughness for Mahe (2010, base case wave conditions).

The absolute runup reduction for Praslin is provided in Figure 5.4. The highest potential runup reduction is shown at Grand Anse, Anse Volbert, and at the priority site of Anse Kerlan near the airport. Baie Ste Anne also shows strong potential runup reduction, but there is greater uncertainty about the measured reef widths here (
Figure *4.10*), so more detailed modelling and in-situ observations of the bathymetry are recommended here.

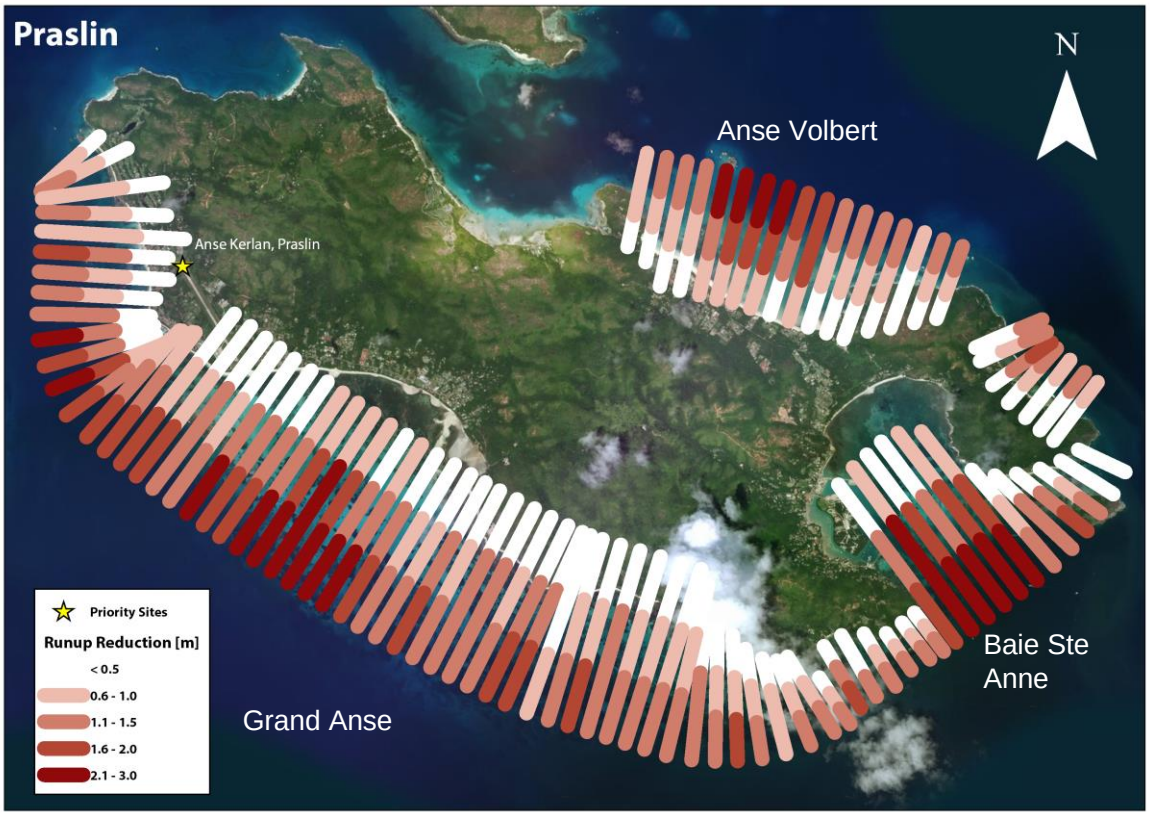

Figure 5.4 Runup reduction as a function of roughness for Praslin (2010, base case wave conditions)

In general, runup reduction shows high spatial variation due to differences in wave climate from island to island, and especially due to the heterogeneous reef geometry (reef depth, width and slopes).

5.3 Runup Reduction as a function of Water Level Increase

The absolute runup reduction was also compared for the three different design water levels provided by the client (1.44 m in 2010, 1.70 m in 2050, and 2.03 m in 2100, see Table 3.1). Water level increases generally result in a vertical translation of the runup, with only minor changes in runup reduction between 2010 and 2100 scenarios (e.g. La Digue in Figure 5.5). In our assessment this is due to the fact that the increase in water depth is small from 2010 to 2100 relative to the 2010 depths (reef depth and 1/25 return period water level). Furthermore, the locations of sites with high runup reduction generally do not shift.

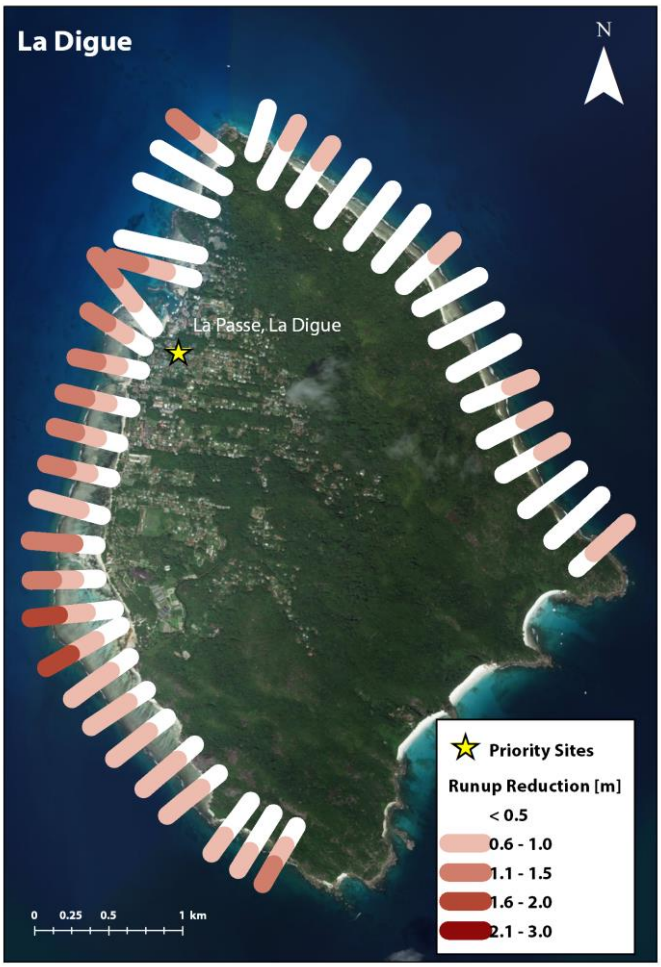

Figure 5.5 Runup reduction as a function of roughness for La Digue (2100, base case wave conditions).

Although the runup reduction is not especially sensitive to the 0.6 m range of water levels examined for this study, it is possible that more extreme sea level rise scenarios could have a nonlinear effect on runup. Future studies should also consider the impact of these higher-end scenarios.

Additional maps for all tested scenarios can be found in Appendix A.

5.4 Runup Reduction as a function of Wave Height

To determine the sensitivity of the results to changes in wave height, we also examined the absolute runup differences for the base case with a wave height decrease and increase of -1 m and +2 m. Larger offshore waves lead to a relatively higher reduction in runup than smaller waves. This is illustrated in the example of Mahe in Figure 5.6.

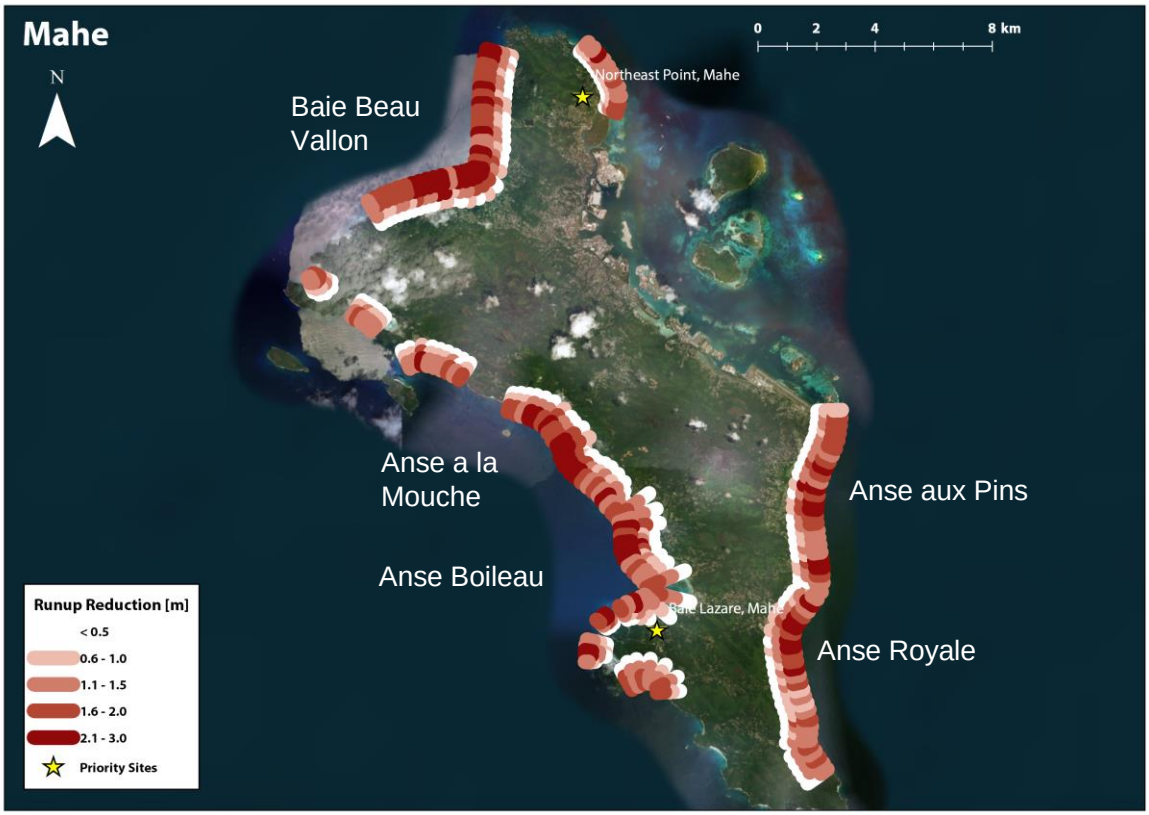

Figure 5.6 Runup reduction as a function of roughness for Mahe (2010, +2 m wave conditions).

Rougher reefs are less sensitive to changes in wave height than smooth ones. Hence, the increase in absolute runup reduction for the no coral minus high coral cover scenario (seaward band in Figure 5.6) is mainly due to increased runup under the no coral scenario for higher waves. The sensitivity of runup to changes in wave height reinforces the need to derive a more comprehensive wave climate in future studies.

Additional maps for all tested scenarios can be found in Appendix A.

6 Discussion

In this section, we compare the results of the quick-scan analysis with a previous investigation by Sheppard et al. (2005). We then discuss limitations of the current approach, data availability and quality.

6.1 Comparison of outcomes with Sheppard et al. (2005)

An investigation of coral health on wave impact on the shoreline by Sheppard et al. (2005) is one of the few studies relating coral coverage to a bottom friction coefficient. As the purpose of our quick-scan is similar to the research goals of the Sheppard paper (but for the entire island), we relate our results to the results of Sheppard at 10 of the 14 locations that were considered in their paper. The four remaining locations are situated around St. Anne Marine National Park, which is not covered by the transects in this quick-scan. An overview of overlapping study sites from 3 other previous studies with Sheppard's location's and the corresponding transect numbers in the current quick-scan are summarized in Table 6.1. Besides the comparison of outcomes between the two studies, these 10 locations also serve as the locations at which we interpret the historical coral coverage in more detail and relate to Sheppard's roughness choices as well as our own.

Table 6.1 Correspondence between study sites in four previous studies and the current quick-scan.

Sheppard (2005) location	***Wilson (2012) sites***	***Goreau (1998) sites***	***Abdulla (2006)***	***Transect number present study***
1	Mahé E	-	-	Mahé_M6_42
2	Mahé NW	-	-	Mahé_M0_28
3	-	North Victoria Harbour mouth	-	Mahé_M7_4
4	Mahé NW	-	l'ilot rocks	Mahé_M0_7
5	Mahé NW	Baye Ternay	Baie Ternay	Mahé_M1_1
6	Mahé W	-	-	Mahé_M2_1
7	Mahé W	-	-	Mahé_M2_11
12	Praslin SW	-	-	Praslin_P2_6
13	Praslin NE	-	-	Praslin_P0_2
14	-	Southwest La Digue	La Digue	La Digue_D0_31

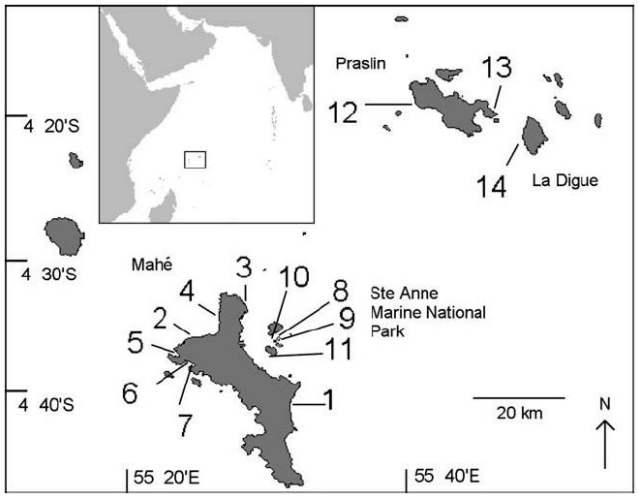

Figure 6.1 Map of the granitic Seychelles islands, showing locations of each reef surveyed in Sheppard (2005). Taken from Sheppard (2005).

6.1.1 Current state of reef roughness

From a flood safety perspective, one of the most important characteristics of a coral reef is the structural complexity of the corals and the coverage percentage, as the roughness is known to reduce wave heights and runup at the shoreline. The coverage percentages are described for a number of areas by Wilson et al. (2012). The coverage percentages per substrate type for each of the relevant areas were averaged assuming all three substrate types were present in equal amount in the study areas, since the Wilson study provided no information on substrate distribution. The complete description of the 1994 state was supplemented with the reported decay and growth percentages to arrive at 2011 coverage percentages. These coverage percentages were associated with roughness classes following Sheppard et al. (2005) (Table 6.2).

Table 6.2 Association of coverage classes in the Bayesian Network to the percentages reported on in Wilson (2012).

	From (%)	To (%)
no	0	5
low	5	25
medium	25	75
full	75	100

Two of the transects under consideration were not covered by Wilson's study. Reference was made to Goreau (1998) and Abdulla (2006) to fill the coverage information (Table 6.3).

Table 6.3 Coverage classes deduced from the literature for 10 transects within the quickscan. All classes are based on Wilson (2012) apart from the grey background coloured values, which are based on Goreau (1998).

Transect Name	Coverage class
Mahé_M6_41-42-43	no
Mahé_M0_28	low
Mahé_M7_4	low
Mahé_M0_7	low
Mahé_M1_1	low
Mahé_M2_1	medium
Mahé_M2_11	medium
Praslin_P2_6	low
Praslin_P0_2	low
La Digue_D0_31	low

6.1.2 Comparison with Proxy for Wave-Induced Flooding

Sheppard's study and the present one differ in their proxy for flood safety (energy at the shoreline vs runup, respectively). As a consequence, the results cannot be compared on a one-to-one basis per transect. The Wilson et al. (2014) wave energies at the shoreline were converted to significant wave heights at the shoreline.

Furthermore, the current BEWARE quick-scan study uses hydrodynamic forcing based on wave climates with a 25-year return period (typically 4-5 m), which are significantly larger than offshore waves than the Sheppard study uses (Hs = 1.25). Dissipation of smaller waves typically leads to smaller wave-induced setup and hence to less runup, and this is nonlinearly influenced by the other parameters such as reef width and offshore water level. Furthermore, the offshore water level in Sheppard's study was 0.85 m+MSL, where the current study works with 25-year return period water levels which are 1.44 m+MSL and above.

Still, the current quickscan results for 2010 are compared with the 2014 coverages deduced in Section 6.1.1 to arrive at 2010 runup estimates (Table 6.4). The correlation between the two proxies over the 10 transects is investigated through both a Pearson and Spearman (ranked) correlation. The correlation between proxies for most flood prone transect is negative ($r = -0.29$). Acknowledging the non-linear relationship between nearshore wave height and runup, the ranked correlation was investigated as well, but this did not lead to a stronger or more positive correlation between the two studies.

Table 6.4 Correlation between flooding proxy significant wave height and runup between current quick-scan and results from Sheppard (2005).

ID	Flooding proxy		Ranks	
	quickscan runup [m]	Sheppard Hs [m]	quickscan	Sheppard
Mahé_M6_42	4.4	0.21	1	1
Mahé_M0_28	5.1	0.6	5	10
Mahé_M7_4	8.4	0.44	8	3.5
Mahé_M0_7	5.1	0.49	4	6.5
Mahé_M1_1	8.8	0.23	9	2
Mahé_M2_1	5.0	0.57	3	9
Mahé_M2_11	6.4	0.49	6	6.5
Praslin_P2_6	8.9	0.44	10	3.5
Praslin_P0_2	6.8	0.45	7	5
La Digue_D0_31	4.8	0.5	2	8
			Spearman's Rho	**Pearson's r**
			-0.34	-0.29

Although Sheppard et al. (2005) is the only available study for the Seychelles that is similar to the current quick-scan, there are fundamental differences in the two methods, input data, output variables, and underlying assumptions which are likely to cause the observed differences. This means that any comparison of results between the two studies should be interpreted with caution.

6.2 Limitations on the method, data availability and data quality

This quick-scan analysis is based on a method which was originally designed for fringing reefs, where the reef geometry was schematized into a uniform foreshore slope, a horizontal reef flat and a plane beach slope. This method has previously been applied and validated on two fringing reef sites (Roi-Namur and Funafuti) in the Pacific, as reported in Pearson et al. (2017a).

The schematization does capture the essential features of a fringing reef, but not the details such as the reef crest and bathymetric complexity. Quataert et al. (2015) investigated the differences between a schematized profile and an in-situ measured profile for a fringing reef in the Marshall Islands, and found that the effect on the runup was very small. The reason is that the wave transformation essentially integrates over the profile, and that local variations do not significantly affect the end result at the beach.

However, there are a few necessary assumptions and thus limitations in the methodology and data availability and quality that warrant attention in the interpretation of the results.

First of all, we applied offshore wave boundary conditions based on scarce data in the literature. This resulted in near uniform wave conditions around the islands (Figure *4.14*), which does not do justice to the wave sheltering and propagation (refraction) processes which are likely to take place around the islands. In order to capture this properly, a wave transformation study using a spectral wave model such as SWAN should be performed, but this was outside the scope of the present study.

Secondly, we apply normally incident, long-crested waves which propagate along the shore-normal transects. Because all wave components travel in the same direction, the infragravity wave (long wave) that is forced by the incoming short waves is amplified maximally. This approach was previously used on Roi-Namur (Quataert et al., 2015), but is likely to give an overestimation of the runup relative to a 2D-horizontal case which would include directionally-spread waves. However, this overestimation results in a conservative (non-optimistic) estimate of the runup which is useful to assess the reduction effect of roughness on the coastal hazard.

Third, the fringing reef schematization into a reef slope, reef flat and beach slope is known to be less applicable on complex topographies which do not resemble fringing type reefs. These non-fringing reef profiles were found especially on the Praslin Island coast, which has very complex gently sloping bays with high apparent bathymetric complexity. Still, for these wider bays we estimate that the large reef widths found are an indicator of the potential to reduce wave runup if the coral reefs in those bays are restored. However, a more detailed study (using for instance a 2D model) is recommended.

Fourth, the reef depth and slope input was derived from remote-sensed data. While the general trends and values correspond reasonably well to the scarce observations, the selected candidate sites should be surveyed in more detail to estimate the depth and slopes. Assessing the ground truth bathymetry, we observe milder fore reef slopes in the upper part which are consistent with the remote-sensed values. However, in some areas the in-situ data has steeper fore reef slopes below the 5 meter depth contour (Figure 6.2) which the satellite data does not register because of depth limitations. Because we schematize the reef with a single fore reef slope we selected the upper slope as the waves will be most affected as the depths become shallower. Moreover, as is shown in Pearson et al. (2017a) the fore reef slope is one of the least controlling parameters on the runup. For the prioritized sites, a more detailed analysis and comparison with in situ measured data should be performed.

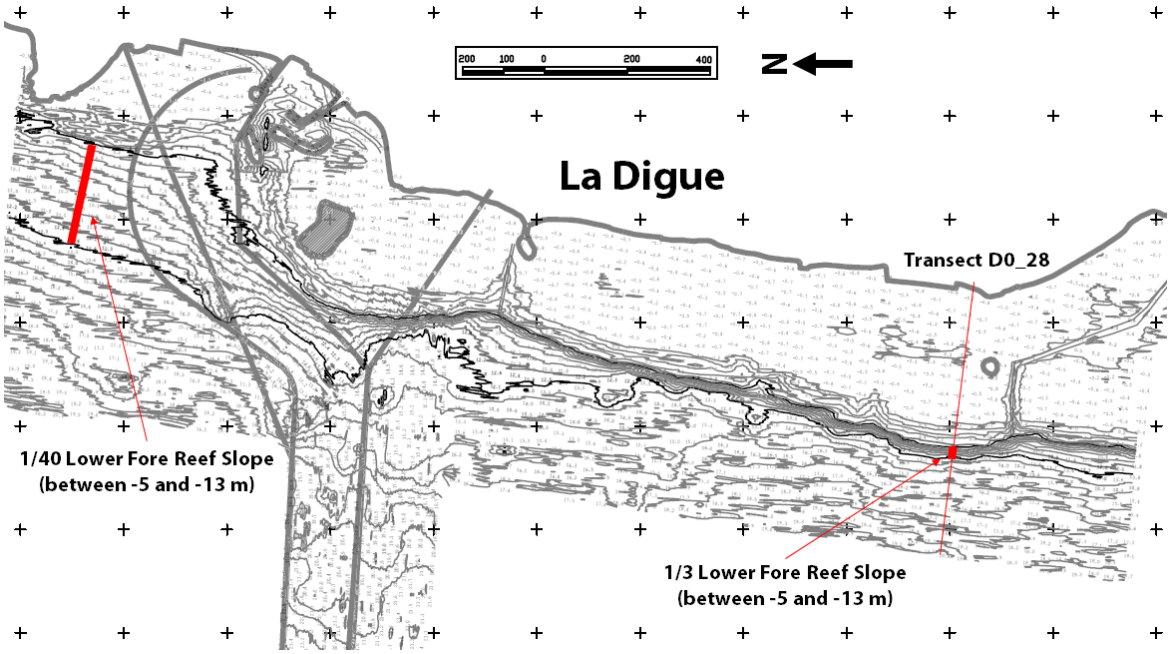

Figure 6.2 Variation in lower fore reef steepness along the west coast of La Digue can be visualized by examining the distance between the -5 and -13 m contours (thick black lines). The southern section of the coast (right side) is much steeper than in the north (left side). However, the upper 5 m of the fore reef shows less alongshore variation.

Fifth, in our study we apply a uniform roughness on the reef flat, while in reality the roughness is spatially heterogeneous. Therefore, this study does not give insight into the effect of a reef restoration with increased roughness in a particular part of the profile. It is thus recommended to investigate in which location on the reef and for which dimensions (in terms of increased roughness and bed elevation) a restoration project will yield the most optimal results in terms of wave runup reduction.

Finally, the Bayesian network (BN) used in this study as part of the BEWARE system was originally developed as a potential early warning system for flooding on reef-lined coasts (Pearson et al., 2017). However, it is also applicable for the present application in determining runup reduction due to increased reef roughness. There are several key advantages to this approach. First, the BN is much faster than a process-based numerical model once the underlying database has been developed. This enables multiple scenarios (e.g. different roughness values or offshore forcing) to be simulated and compared quickly. Second, unlike deterministic process-based models, BNs are also able to take account for uncertainty of input variables, and to express uncertainty in their outputs using probability distributions. However, a detailed assessment of these probability distributions was beyond the scope of the quick-scan analysis, and only an expected value was returned. A disadvantage of this type of BN is that it returns output in a discretized form (in bins), rather than an exact value. However, by using bins significant changes in runup reduction due to increased roughness are more clearly demonstrated. BNs are also data-intensive, which in this case meant that tens of thousands of model simulations are required to make predictions across the given parameter space.

7 Description of digital output products

This report is accompanied by a digital dataset consisting of a spatial dataset that depicts relative run-up and other parameters for Mahé, Praslin and La Digue.

a. Description of the data attributes:

- (2%) run-up under three different selected offshore wave conditions;
- Additional intermediate data on the reef input parameters (reef width, reef slope, beach slope, and reef roughness);
- Absolute reductions in runup (no-high, no-medium and no-low)
- Relative reductions in runup ((no-high/no), (no-medium)/no, (no-low)/no)
- Quality control flags.

b. Appendix with 54 runup reduction maps for each island for:

- Absolute and relative runup changes for all three islands
- Three waterlevels (2010, 2050, 2100)
- Three wave conditions (base wave height, waveheight-1 m, waveheight +2 m)

b. Format

- All data will be delivered via an online transfer
- All data delivered in shapefile
- Folder structure:
    - Shp
        - Reef Properties
        - Model Inputs & Results
        - Runup Reduction
        - Quality Control
    - All shapefiles are organized by island. Letters A-C indicate the position used for plotting (A is seaward, C is landward).

8 Conclusions

The objective of this study is to perform a quick-scan analysis for three islands of the Seychelles (Mahé, Praslin and La Digue) to identify candidate sites which have a high potential for the reduction of wave runup through coral reef restoration. Wave runup is selected as a proxy for coastal flooding levels.

The analysis was carried out using remote sensing and existing (but limited in coverage) datasets to estimate key site parameters such as reef width, depth, fore reef slope roughness, and beach slope. Hydrodynamic forcing was derived from literature and provided 1/25 year return periods for the wave conditions and water levels at current conditions and including sea level rise.

On this basis, 40,000 combinations of forcing and geometric parameters were input in the wave transformation model XBeach to compute the associated runup. The input and model response were used to train a Bayesian Network, and this network was then used to provide a runup estimate for each of the more than 300 defined transects for four values of reef roughness corresponding to no coral cover, low cover, medium cover and high cover.

In general, a low coral cover offers little benefit relative to medium or high coral cover. For La Digue, the results show that the wave reduction potential is generally higher on the western side as the reefs are wider than on the east side. Highest potential reductions are found near the client's priority site of La Passe but also at Anse Union which has a wide and shallow reef. At Mahé, we find a number of locations in concave parts of the coast (which are generally associated with wider reefs) on the eastern and western shore: Anse Royale, Anse aux Pins, Baie Beau Vallon and Anse a la Mouche, and to some extent the identified priority area of Baie Lazare. The priority area at Anse Nord D'Est shows some potential, but the results are quite variable in the alongshore direction at that location. The reefs around the island of Praslin were least like the fringing reef types for which the method was designed for. Therefore, the results are most uncertain since reef edges were not easy to define. From the results of Praslin, we find that the bays at Grand Anse and Anse Volbert which from the results and by visual inspection have the largest (but uncertain) widths have the most potential. The client's priority site at Anse Kerlan was confirmed to have reduction potential. The south-eastern Baie St. Anne showed also some potential, but this appears to be a wide and shallow bay where the present method is very uncertain about the geometry.

We find that the reef reduction potential is not very sensitive to an increase in the 1/25 return period water levels, as the projected increase from present to 2100 is small relative to the current total water depth under 1/25 year return conditions. We do find a large effect due to a change in offshore wave height. The runup for the cases of high reef roughness is not very sensitive to offshore wave height variations, but the runup for the cases of no or low roughness is. Hence, as the wave height increases, the absolute differences between high and no (or low) roughness increases as well. This is a testimony to the protective value of healthy, rough reefs.

9 Recommendations

The results presented in this study are based on a quick-scan study which is subject to a number of assumptions and simplifications. These were necessary in order to perform the analysis, and the results are useful to prioritize sites.

However, before implementation of coral reef restoration schemes, it is recommended to perform more detailed analyses:

- First, we recommend to better estimate the offshore wave climate around the islands using a numerical wave model such as SWAN, as the currently used climate from the literature is quite alongshore uniform.
- Also, for the priority sites the assumption of shore-normal incident long-crested waves should be released by applying a 2D wave transformation model such as XBeach. This is a computationally feasible option for these smaller islands.
- Furthermore, the remote-sensed estimations of reef depth and extent should be verified in the field. Moreover, the distribution of the present coral cover, which could not be assessed for all islands' coasts, should be verified from aerial photography or the literature.
- Finally, a numerical study could give insight into the optimal location and extent of a coral restoration scheme on a reef platform.

10 Bibliography

Abdulla, A., Bijoux, J., Engelhardt, U., Obura, D., Payet, R., Pike, K., ... & Skewes, T. (2005). 10. Status of the coral reefs of the Seychelles after the December 2004 tsunami.

Baldock, T. E., Golshani, A., Callaghan, D. P., Saunders, M. I., & Mumby, P. J. (2014). Impact of sea-level rise and coral mortality on the wave dynamics and wave forces on barrier reefs. Marine pollution bulletin, 83(1), 155-164.

Beck, M. W., Losada, I. J., Menéndez, P., Reguero, B. G., Díaz-Simal, P., & Fernández, F. (2018). The global flood protection savings provided by coral reefs. Nature communications,9(1), 2186.

Booij, N. R. R. C., Ris, R. C., & Holthuijsen, L. H. (1999). A third-generation wave model for coastal regions: 1. Model description and validation. *Journal of geophysical research: Oceans*, *104*(C4), 7649-7666.

Borrero, J.C., Atkin, E.A., Greer, D., O'Neill, S.M., Mead, S.T. (2016) Coastal Processes Study: North East Point, Mahé Island, Seychelles. eCoast. Ragland, New Zealand.

Chong-Seng, K. M., Graham, N. A. J., & Pratchett, M. S. (2014). Bottlenecks to coral recovery in the Seychelles. Coral reefs, 33(2), 449-461.

DeMers, M. N. (2008). Fundamentals of geographic information systems. John Wiley & Sons.

Hagenaars, G., de Vries, S., Luijendijk, A. P., de Boer, W. P., & Reniers, A. J. (2018). On the accuracy of automated shoreline detection derived from satellite imagery: A case study of the Sand Motor mega-scale nourishment. Coastal Engineering, 133, 113-125.

Harris, D. L., Rovere, A., Casella, E., Power, H., Canavesio, R., Collin, A., ... & Parravicini, V. (2018). Coral reef structural complexity provides important coastal protection from waves under rising sea levels. Science advances,4(2), eaao4350.

Goreau, T. (1998). Coral bleaching in The Seychelles Impacts and Recommendations. Preliminary Report, 1-9

Grohmann, C. H., & Riccomini, C. (2009). Comparison of roving-window and search-window techniques for characterising landscape morphometry. *Computers & Geosciences*, *35*(10), 2164-2169.

Graham, N. A., Wilson, S. K., Jennings, S., Polunin, N. V., Bijoux, J. P., & Robinson, J. (2006). Dynamic fragility of oceanic coral reef ecosystems. Proceedings of the National Academy of Sciences, 103(22), 8425-8429.

Graham, N. A., Wilson, S. K., Jennings, S., Polunin, N. V., Robinson, J. A. N., Bijoux, J. P., & Daw, T. M. (2007). Lag effects in the impacts of mass coral bleaching on coral reef fish, fisheries, and ecosystems. Conservation biology, 21(5), 1291-1300.

Graham, N. A., Jennings, S., MacNeil, M. A., Mouillot, D., & Wilson, S. K. (2015). Predicting climate-driven regime shifts versus rebound potential in coral reefs. Nature, 518(7537), 94.

Japan International Cooperation Agency. (2014). The Study for Coastal Erosion and Flood Control Management in the Republic of Seychelles.

Lillesand, T., Kiefer, R. W., & Chipman, J. (2014). *Remote sensing and image interpretation*. John Wiley & Sons.

Pacheco, A., Loureiro, C., Horta, J., & Ferreira, Ó. (2015). Retrieval of nearshore bathymetry from Landsat 8 images: A tool for coastal monitoring in shallow waters. Remote Sensing of Environment, 102-116.

Pearson, S. G., Storlazzi, C. D., van Dongeren, A. R., Tissier, M. F. S., & Reniers, A. J. H. M. (2017a). A Bayesian-Based System to Assess Wave-Driven Flooding Hazards on Coral Reef-Lined Coasts. Journal of Geophysical Research: Oceans,122(12), 10099-10117.

Pearson, S.G., Storlazzi, C.D., van Dongeren, A.R., Tissier, M.F.S., Reniers, A.J.H.M. (2017b). BEWARE database: A Bayesian-based system to assess wave-driven flooding hazards on coral reef-lined coasts: U.S. Geological Survey data release, https://doi.org/10.5066/F7T43S20.

Quataert, E., Storlazzi, C., Rooijen, A., Cheriton, O., & Van Dongeren, A. (2015). The influence of coral reefs and climate change on wave-driven flooding of tropical coastlines. Geophysical Research Letters, 42(15), 6407-6415.

Roelvink, D., Reniers, A., van Dongeren, A. R., de Vries, J. V. T., McCall, R., & Lescinski, J. (2009). Modelling storm impacts on beaches, dunes and barrier islands. Coastal engineering, 56(11-12), 1133-1152.

Roelvink, D., McCall, R., Mehvar, S., Nederhoff, K., & Dastgheib, A. (2018). Improving predictions of swash dynamics in XBeach: The role of groupiness and incident-band runup. Coastal Engineering, 134, 103-123.

Sheppard, C., Dixon, D. J., Gourlay, M., Sheppard, A., & Payet, R. (2005). Coral mortality increases wave energy reaching shores protected by reef flats: examples from the Seychelles. Estuarine, Coastal and Shelf Science, 64(2-3), 223-234.

Smit, P. B., Stelling, G. S., Roelvink, D., van Thiel de Vries, J., McCall, R., van Dongeren, A., ... & Jacobs, R. (2010). XBeach: Non-hydrostatic model. Report, Delft University of Technology and Deltares, Delft, The Netherlands.

Wilson, S. K., Graham, N. A., Fisher, R., Robinson, J., Nash, K., Chong-Seng, K., ... & Quatre, R. (2012). Effect of macroalgal expansion and marine protected areas on coral recovery following a climatic disturbance. Conservation Biology, 26(6), 995-1004.

Deltares

Enabling Delta Life

GFDRR

Global Facility for Disaster Reduction and Recovery

THE WORLD BANK

IBRD • IDA | WORLD BANK GROUP